Nanoscale

ROYAL SOCIETY OF CHEMISTRY

MINIREVIEW

View Article Online
View Journal | View Issue

Cite this: *Nanoscale*, 2025, **17**, 22100

Unravelling the nanoarchitectonics of –C–N– linkages in covalent organic frameworks for CO_2 capture—a mini-review

Princy Deni Raju, * Athira Rajasekharan Sujatha, Saumya Krishnan and Chettiyam Veettil Suneesh *

Covalent Organic Frameworks (COFs) featuring carbon–nitrogen (C–N) linkages represent a versatile class of crystalline, porous materials constructed through the dynamic covalent bonding of organic monomers. Schiff-base, C–N imine-linked COFs have garnered considerable interest for carbon dioxide (CO_2) capture owing to their highly tunable structures, excellent thermal and chemical stability, and enduring porosity, which stem from their robust architectures and nitrogen-rich composition. The inherent polarity and Lewis basicity of C–N bonds promote strong CO_2 adsorption *via* dipole-quadrupole and hydrogen bonding interactions, enhancing uptake and selectivity, particularly under low-pressure or humid conditions, making them ideal for real-world applications in CO_2 capture. Key structural attributes, such as nanoarchitectures based on small pore sizes, electron-rich substituents, and three-dimensional multi-layered frameworks, further enhance both stability and CO_2 affinity by reinforcing π-conjugation and improving weak supramolecular interactions. This mini-review delves into the mechanistic role of C–N connectivity in influencing CO_2 gas affinity and framework stability, highlighting a promising pathway for the rational design of next-generation COFs for carbon dioxide capture and storage technologies.

Received 31st May 2025,
Accepted 2nd September 2025

DOI: 10.1039/d5nr02324f

rsc.li/nanoscale

1. Introduction

Greenhouse gases (GHGs), which trap heat at the Earth's surface, play a crucial role in maintaining the planet's energy balance and supporting life. In the absence of these gases, the global average surface temperature would be approximately 32.5 °C lower than the current average of 14.4 °C, resulting in an estimated temperature of −18 °C.[1] However, elevated con-

Department of Chemistry, University of Kerala, Kariavattom Campus, Thiruvananthapuram-695581, Kerala, India.
E-mail: princydeniraju@keralauniversity.ac.in, suneesh@keralauniversity.ac.in, suneeshcv@gmail.com

Princy Deni Raju

Princy Deni Raju is currently pursuing her PhD in the Department of Chemistry at the University of Kerala. She previously earned her Bachelor of Science (B.Sc.) in Chemistry from Mahatma Gandhi University and her Master of Science (M.Sc.) in Chemistry from the University of Kerala. Her research focuses on the development of porous organic polymers for CO_2 gas adsorption, energy storage and catalytic applications.

Athira Rajasekharan Sujatha

Athira Rajasekharan Sujatha is currently pursuing her PhD in the Department of Chemistry at the University of Kerala. She previously earned her B.Sc. (Bachelor of Science) M.Sc. (Master of Science), and M.Phil. (Master of Philosophy) in Chemistry from the same university. Her research is centered on the synthesis of porous organic polymers, particularly covalent organic frameworks (COFs) and conjugated microporous polymers (CMPs), with an emphasis on energy applications.

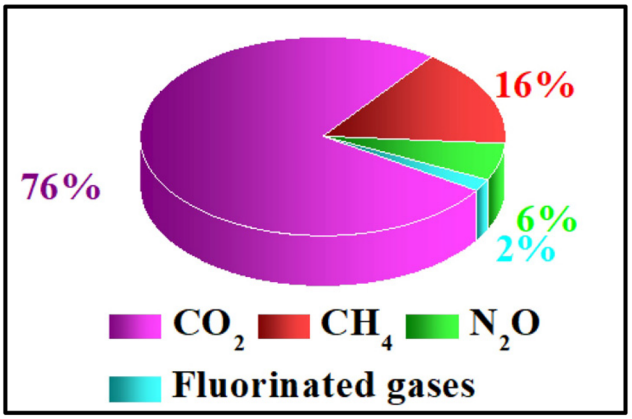

Fig. 1 Source: forcing greenhouse gases – Global emissions (2012), International Energy Agency.

centrations of GHGs – such as carbon dioxide (CO_2), nitrous oxide (N_2O), methane (CH_4), water vapour (H_2O), and fluorinated gases – pose significant challenges to sustainable development.[2,3] According to the Intergovernmental Panel on Climate Change (IPCC) Sixth Assessment Report, radiative forcing – defined as the change in net radiative flux (W m^{-2}) due to drivers such as CO_2 emissions, volcanic aerosols, and variations in solar output – is a key metric in assessing climate impact.[4,5] Since the 1980s, CO_2-induced radiative forcing has increased by approximately 57%, and CO_2 currently accounts for about 80% of the total radiative forcing attributed to GHG emissions.[2,6] As illustrated in Fig. 1, rising atmospheric CO_2 concentrations are the primary driver of contemporary climate change. Recent studies by the European Chemical Industry Council propose that CO_2 utilized in fuel production and other short-lived applications can be classified as "negative emissions", regardless of its source or sequestration pathway.[7,8]

According to the 2023 annual report from the National Oceanic and Atmospheric Administration (NOAA) Global Monitoring Laboratory, the global average atmospheric CO_2 concentration reached 419.3 ppm.[9] This rise in atmospheric CO_2 is of critical concern for two main reasons. First, CO_2 is the most impactful anthropogenic greenhouse gas, with a strong capacity to absorb and re-radiate infrared radiation, unlike diatomic gases such as oxygen and nitrogen. The continuous increase in CO_2 concentration, primarily driven by human activities, is directly linked to the rise in global temperatures.[10] Second, CO_2 readily dissolves in ocean water, forming carbonic acid and contributing to ocean acidification – a process that alters marine chemistry and threatens aquatic ecosystems.[11]

Given these environmental consequences, the development of effective CO_2 capture and conversion technologies is imperative to mitigate atmospheric CO_2 levels and reduce associated ecological risks. Historically, anthropogenic CO_2 emissions began to escalate significantly during the Industrial Revolution, initiated around 1750 with the advent of steam power. The large-scale combustion of fossil fuels – initially coal, followed by oil and natural gas – has since accelerated the release of CO_2 into the atmosphere. To limit global warming and meet the objectives outlined in the Paris Agreement, it is essential to implement sustainable strategies aimed at reducing global CO_2 emissions by 45% by 2030 and achieving net-zero emissions by 2050.[12] Fig. 2 presents normalized annual CO_2 emissions from fossil fuel combustion and industrial activities. Additionally, the figure highlights the regional contribution from Asia (Fig. 2b), illustrating the exponential increase in CO_2 emissions over recent decades.

Technologies enabling the efficient utilization of CO_2 are critical to establishing a sustainable, circular carbon economy, where CO_2 is treated as a valuable resource rather than a waste

Saumya Krishnan

Dr Saumya Krishnan was awarded Master of Science in Chemistry from University of Kerala in 2012 and M. Phil. in Chemistry from University of Kerala in 2015. She received his PhD from University of Kerala, in 2021. Later she worked as a postdoctoral fellow in University of Kerala (2022–2023) and worked as Assistant Professor (Contract) in various colleges. Her research focuses on the organic porous organic polymers for various applications.

Chettiyam Veettil Suneesh

Dr Chettiyam Veettil Suneesh was awarded Master of Science in chemistry from University of Calicut. He received his PhD from Cochin University of Science and Technology, India in 2010, working at CSIR-National Institute of Interdisciplinary Science and Technology. During PhD, he has a short stay at Lehigh University, USA as a DST-NSF visiting fellow. Later he worked as a postdoctoral research associate in Kyushu University Japan (2010–2012). Then he joined the University of Kerala, India in 2012 and is currently an Assistant Professor at the department of chemistry there. His research focuses on the organic luminescent molecules and porous organic polymers for various applications.

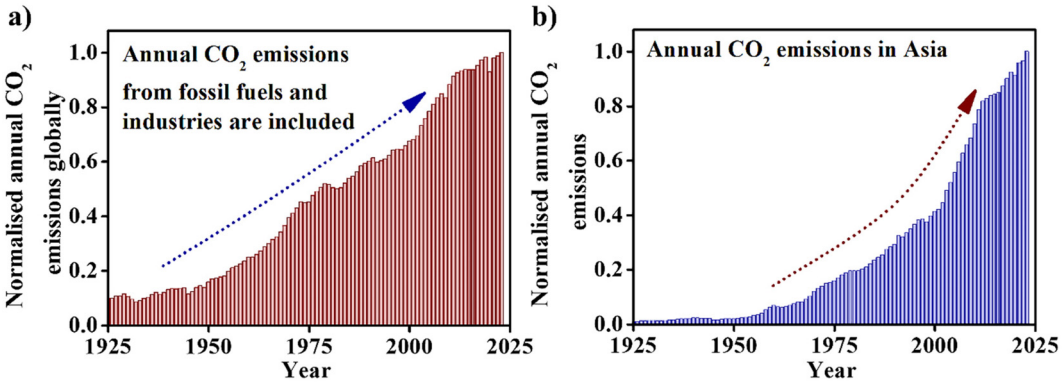

Fig. 2 (a) Annual CO_2 emission data from fossil fuels and industries globally (divided the values with maximum value obtained 37.79 billion tonnes). (b) Annual CO_2 emissions in whole region of Asia (divided the values with maximum value obtained 19.75 billion tonnes). Source: Global Carbon Budget (2024).

product. As such, carbon dioxide utilization is considered a viable short- to mid-term strategy for mitigating atmospheric CO_2 levels due to its relatively straightforward implementation. The three principal CO_2 mitigation approaches include pre-combustion,[13] post-combustion,[14] and oxy-fuel combustion methods.[15] A comparison of the key advantages and disadvantages of different approaches is discussed in Table 1. In conjunction, five major CO_2 separation techniques have been developed: chemical looping,[16] membrane separation, adsorption, absorption, and cryogenic distillation.[17,18] Table 2. provides a comparison of the main merits and demerits of various approaches. Among these, adsorption-based systems have gained significant attention due to their high CO_2 uptake capacities, low energy requirements, and reduced operational and maintenance costs.[19] The development of efficient, porous adsorbent materials that demonstrate high selectivity for CO_2 in the presence of other gases has thus become a research priority.

Adsorbents are generally classified into low-temperature and high-temperature categories. High-temperature materials, such as reactive metal oxides (*e.g.*, hydrotalcites and calcium oxide), are not considered within the scope of this article.[30] Low-temperature adsorbents can be further categorized as chemisorbents or physisorbents. Chemisorbents typically include amine-functionalized materials supported on oxides, polymers, or metal–organic frameworks (MOFs), while physisorbents comprise zeolites, MOFs, activated carbons, and related porous compounds.[31] Porous materials are characterized by a network of voids, with pore sizes ranging from micropores (<2 nm), mesopores (2–50 nm), to macropores (>50 nm), facilitating gas diffusion and molecular separation.[32] MOFs, in particular, have emerged as promising materials due to their

Table 1 Merits and demerits of different CO_2 mitigation approaches

CO_2 capture methods	Merits	Demerits
Post-combustion	(a) It can capture CO_2 from flue gases with low concentrations of CO_2 (typically 10–15%).[20]	(a) CO_2 is captured from a low-pressure (1 bar) gas stream with low CO_2 content (3%–20%), often at high temperatures (120–180 °C), and containing impurities such as SO_x and NO_x.[21]
	(b) Use of activated carbon as one of the adsorbents makes the process environmentally friendly.[22]	
	(c) Captured CO_2 can be utilized for a variety of purposes, such as enhanced oil recovery (EOR) or as a feedstock for chemical production, making the process more economically viable.[13]	
Pre-combustion	(a) Useful in CO_2 capture at high pressure and concentrated gas streams, leading to carbon-free fuel.[23]	(a) High costs and increased risks limit the process.[23]
	(b) Key adsorbents include zeolites, metal–organic frameworks (MOFs), carbon molecular sieves, and various polymer-based materials.[20]	
	(c) Syngas, the main product of pre-combustion capture, can be used in combined cycle power generation or as a feedstock for producing various chemicals.[24]	
Oxy-fuel combustion	(a) Oxy-fuel combustion results in a significant reduction in NO_x emissions.[25]	(a) A major drawback of oxy-fuel combustion is the energy-intensive air separation process required.[25]
	(b) Compared to other CO_2 removal technologies, purifying the stream is easier once trace contaminants have been removed.[20]	

Table 2 Merits and demerits of different CO_2 separation techniques

CO_2 separation techniques	Merits	Demerits
Chemical looping	(a) It has lower energy requirements because it does not need solvent regeneration or a separate air separation unit.[26]	(a) The oxygen carrier used in chemical looping may undergo deactivation over time due to carbon deposition, sintering, or oxidative wear.[26]
	(b) It uses a reusable oxygen carrier that cycles through reduction and oxidation states, which is more energy-efficient and stable.[26]	
Membrane separation	(a) High separation efficiency and high selectivity over other gases.[23]	(a) Limited CO_2 purity.[27]
		(b) Lower efficiency at higher CO_2 concentrations.[27]
Adsorption	(a) Suitable for temperature or pressure swing adsorption operations – low energy consumption and reduced operational and maintenance costs.[20]	(a) Scale-up challenges and the cost of adsorbent materials can hinder large-scale deployment.[28]
	(b) Adsorbents can often be regenerated by pressure or temperature changes, making them reusable for multiple cycles.[28]	(b) Limited CO_2 storage capacity.[29]
Absorption	(a) Absorption processes, especially amine scrubbing, exhibit high selectivity for CO_2, effectively separating it from other gases, even in diluted streams.[23]	(a) The removal of CO_2 for the regeneration of the absorbent is energy-demanding process compared to that of adsorption techniques.[23]
		(b) Solvent degradation over time leads to corrosion, which increases the maintenance and costs.[23]
Cryogenic distillation	(a) Separation of CO_2 from streams having high CO_2 concentrations.	(a) Cryogenic distillation requires large and bulky equipment.[23]
	(b) No chemical reagents.[23]	

structural tunability and dual-mode interaction with CO_2. Depending on their functionalization and framework design, MOFs can exhibit both chemisorptive and physisorptive behavior, making them highly versatile candidates for CO_2 capture from flue gases and other emission sources.[33,34]

Metal–organic frameworks are a class of crystalline materials composed of metal nodes coordinated with organic ligands, forming highly porous, extended network structures.[35] The concept of linking molecular building blocks *via* strong covalent bonds to yield either amorphous or crystalline materials was pioneered by Omar M. Yaghi, who later extended this approach to create MOFs and Covalent Organic Frameworks (COFs).[36] In 1995, O. M. Yaghi *et al.* reported the first MOFs by integrating the microporosity and crystallinity of zeolites with metal–organic linkages, marking a significant advancement in porous materials chemistry.[37] Since their discovery, MOFs have gained widespread attention due to their high surface area, tunable pore sizes, and structural versatility, positioning them at the forefront of applications such as gas separation,[38] catalysis,[39] sensing,[40] and energy storage.[41] Despite these advantages, certain limitations – such as moisture sensitivity, complex synthesis, and limited mechanical stability – can restrict their practical deployment. In contrast, porous organic polymers (POPs) offer superior thermal and chemical stability, more facile synthesis, and greater mechanical flexibility.[42] However, POPs are generally amorphous, in contrast to the crystallinity of MOFs, which can be a disadvantage in applications requiring ordered frameworks. Over the past two decades, several subclasses of POPs have emerged, including hypercrosslinked polymers (HCPs, developed in 1980),[43] polymers of intrinsic microporosity (PIMs, 2004),[44] covalent organic frameworks (COFs, 2005),[45] conjugated microporous polymers (CMPs, 2007),[46] and porous aromatic frameworks (PAFs, 2009).[47] The increase in research activity in this area is reflected in the growing number of publications related to porous materials for gas adsorption, as shown in Fig. 3(a–c).

Among these, covalent organic frameworks have gained considerable interest as promising candidates for CO_2 capture and conversion due to their modularity, thermal and chemical robustness, and well-defined porosity. COFs are crystalline porous materials constructed from light elements such as carbon, hydrogen, nitrogen, oxygen, and boron, linked *via* covalent bonds to form extended, periodic frameworks.[48–52] Their well-ordered structures, functional tunability, and high surface areas render them suitable for a wide range of applications.[53–59] The first COF was reported by A. P. Cote *et al.* in 2005, using borate linkages formed through the self-condensation of 1,4-phenylenediboronic acid.[45] In conventional COF synthesis, reversible interactions facilitate the self-correction of structural misalignments, thereby promoting higher crystallinity. However, in systems dependent on irreversible bonds, the inability to self-correct significantly complicates the formation of well-ordered and highly crystalline structures.[60] Nevertheless, B. Zhang *et al.* synthesised dioxin-linked irreversible COF from linear tetrafluorophthalonitrile (TFPN) and 2,3,5,6-tetrafluoro-4-pyridinecarbonitrile (TFPC), with triangular 2,3,6,7,10,11-hexahydroxytriphenylene (HHTP), which has excellent chemical stability.[61] Later, Y. Su *et al.* developed stable cyano-substituted benzofuran-linked COFs through irreversible cascade reactions.[62] Despite its chemical stability in irreversible COFs, the majority of COFs are produced through reversible covalent bonding. Consequently, the advancement of irre-

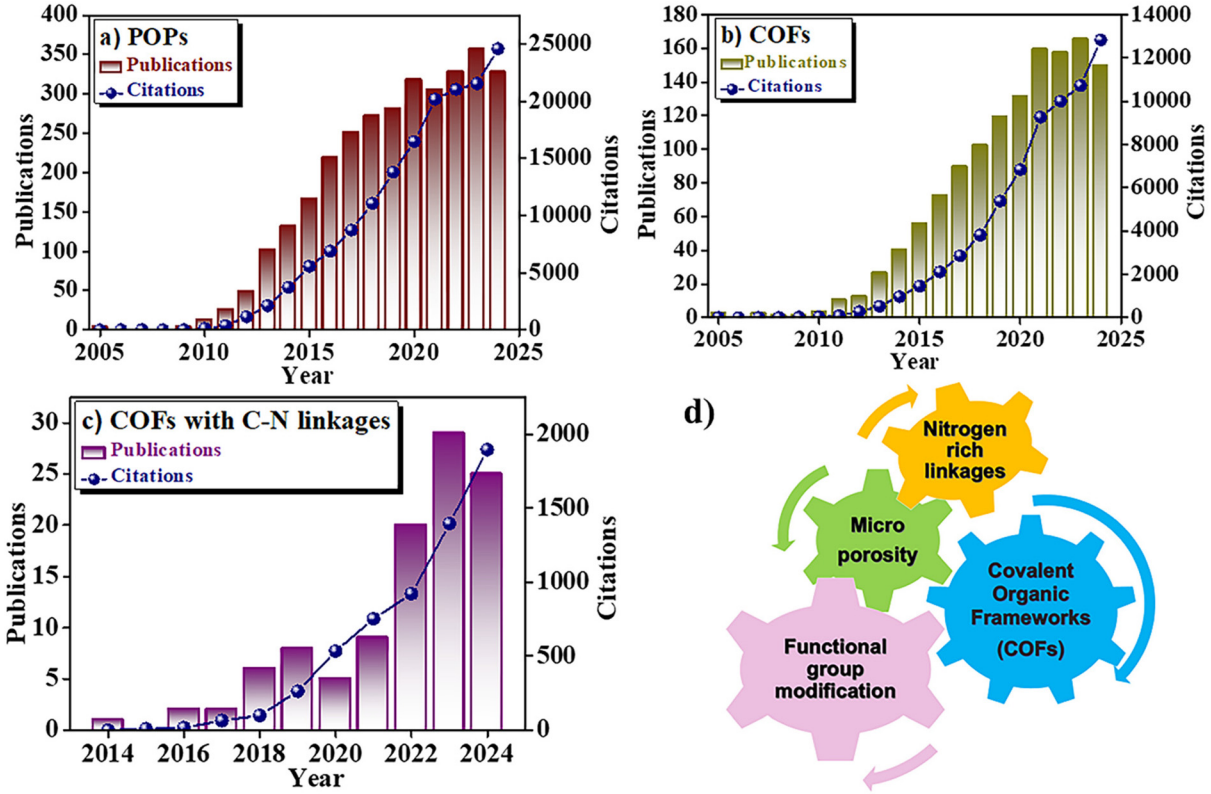

Fig. 3 (a) Annual publications and citations of Porous Organic Polymers (POPs). (b) Covalent Organic Frameworks (COFs). (c) Covalent Organic Frameworks (COFs) with C–N linkages for CO_2 capture over the past 20/10 years (data collected from Web of Science). (d) Designed properties of COFs for CO_2 capture.

versible bonding chemistry in COFs is promising, but it remains a time- and energy-demanding process.[60] This necessitates fine control over reaction kinetics and conditions, such as mild temperatures and pressures, making COF synthesis inherently more challenging than other POPs.[63,64] COFs have been explored for numerous applications, including gas storage and separation,[65,66] catalysis,[67,68] optoelectronics,[69] chemical sensing,[70–73] water purification,[74] energy storage and conversion,[75,76] and biomedical uses such as drug delivery.[77–79] In the context of environmental sustainability, COFs offer significant potential for CO_2 capture, particularly through functionalization and porosity strategies that enhance CO_2-philic behaviour (Fig. 3d).

The COVID-19 pandemic, while temporarily reducing global CO_2 emissions, also highlighted the need for long-term strategies to address climate change. It presented an opportunity to reassess global energy systems, urban infrastructure, and material technologies. In this regard, COFs have emerged as a sustainable solution, particularly due to their adaptability and efficiency in CO_2 capture and conversion. In celebration of the 20th anniversary of COFs, this mini-review highlights recent advancements in COFs featuring enriched nitrogen content through C–N linkages. We explore their design strategies, mechanisms of interaction with CO_2, and their potential as high-performance adsorbents for carbon capture.

2. Historical background

The pioneering work by Furukawa and Yaghi in 2009 represented a significant milestone in the application of covalent organic frameworks for CO_2 capture. Their systematic investigation demonstrated the strong correlation between CO_2 adsorption capacity and structural features (structures are illustrated in Fig. 4), particularly surface area and microporosity. The study concluded that micropore volume is a critical determinant of CO_2 uptake, highlighting the role of pore architecture in enhancing gas storage performance.[65] Subsequent advancements have focused on functional modifications to improve selectivity and adsorption efficiency. In 2015, Q. Gao *et al.* synthesized a nitrogen-rich imine-linked COF using 1,3,5-triformylbenzene and 2,4,6-tris(4-aminophenyl)-1,3,5-triazine under solvothermal conditions. The high nitrogen content in the framework enhanced CO_2 selectivity over CH_4 and N_2 due to favorable interactions with CO_2 molecules.[80] In 2016, L. Wang *et al.* incorporated thiadiazole units into an imine-linked COF through Schiff-base condensation. Thiadiazole, a dipolar heterocycle, offers strong dipole–quad-

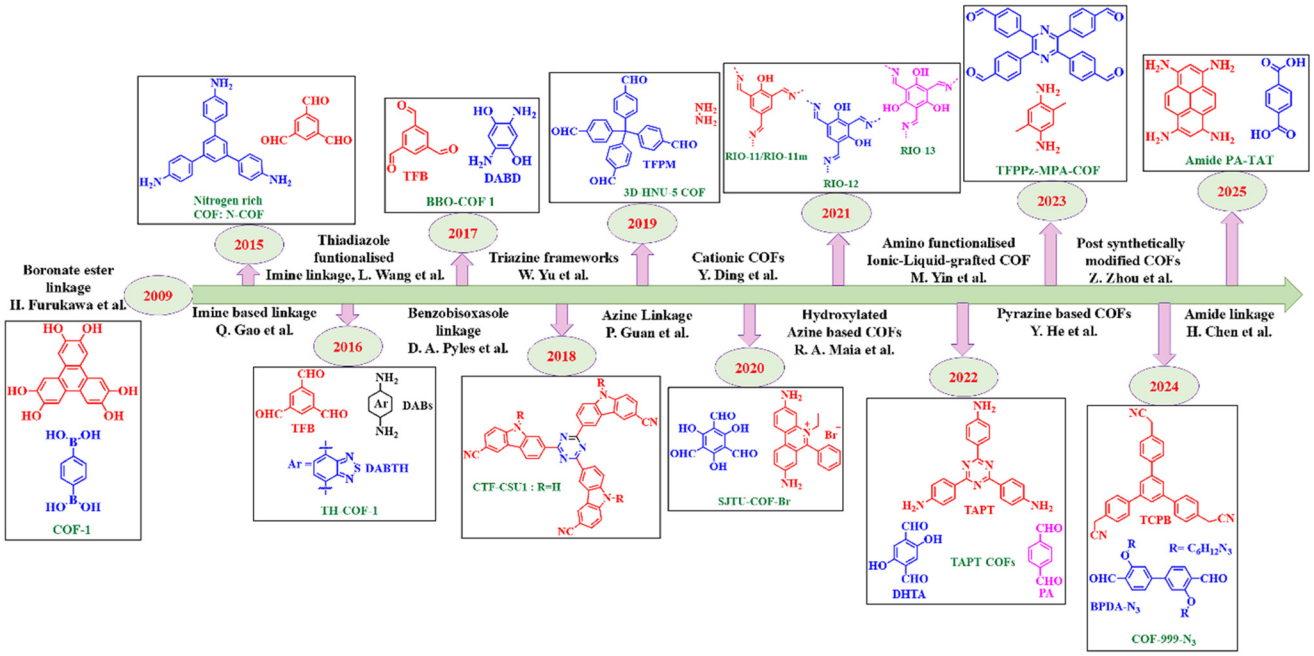

Fig. 4 Progression of Covalent Organic Frameworks (COFs) with various monomers for CO_2 capture over the past decade. This chart illustrates the evolution and advancements in COF design, highlighting the diversity of materials used in CO_2 sequestration.

rupole interactions with CO_2, whose quadrupolar nature results in enhanced adsorption. Additionally, the functional group induced ultra-microporosity (<0.7 nm), facilitating efficient pore-filling at low pressures.[81] In 2017, D. A. Pyles *et al.* reported the synthesis of benzobisoxazole-linked COFs (BBO-COFs) using C_2-symmetric *o*-aminophenol and C_3-symmetric formyl building blocks, catalyzed by cyanide ions. These COFs demonstrated not only substantial CO_2 uptake but also excellent water stability, marking the first successful synthesis of ordered BBO-based COFs.[82] The following year, W. Yu *et al.* developed mesoporous COFs (CTF-CSUs) *via* ionothermal polymerization of triazine- and carbazole-based monomers using $ZnCl_2$ as a catalyst. The presence of nitrogen-rich triazine and carbazole units significantly enhanced the CO_2 capture capacity of the frameworks.[83]

In recent years, the development of three-dimensional (3D) Covalent Organic Frameworks (COFs) has gained significant attention due to their unique structural properties and promising applications in areas such as CO_2 capture and gas storage.[84] Unlike traditional two-dimensional (2D) COFs, 3D COFs exhibit interconnected networks that enhance their stability, adsorption capacity, and exceptional surface area.[84] Recently, H. M. El-Kaderi *et al.* studies have introduced new 3D COFs, such as COF-102, COF-103, COF-105, and COF-108, which are synthesized through the self-condensation of boronic acids to form boroxine rings and co-condensation with catechol to produce boronate ester rings.[85] These frameworks represent a significant advancement in the design of highly functional materials for industrial-scale applications. In 2019, P. Guan *et al.* synthesized a novel 3D azine-linked COF (3D-HNU5) with a two-fold interpenetrated diamond topology *via* room-temperature condensation of tetrakis(4-formylphenyl)methane and hydrazine. Recyclability studies confirmed the material's stability and consistent CO_2 adsorption capacity over multiple cycles, supporting its potential for practical deployment.[86] Y. Ding *et al.* explored the effect of counter anions on CO_2 adsorption in cationic COFs for the first time in 2020. They synthesized a series of anion-exchanged COFs (SJTU-COF-Br, -Cl, -AcO, -CF_3SO_3) *via* microwave-assisted solvothermal methods. Among these, SJTU-COF-AcO exhibited the highest CO_2 uptake, attributed to the interaction between CO_2 and the acetate anion. This interaction, characterized as mild charge transfer between the carbon atom of CO_2 (a Lewis acid) and the oxygen atom of the carboxylate group (a Lewis base), demonstrates the potential of anion exchange as a strategy to tailor COF adsorption properties.[87] Next year, R. A. Maia *et al.* synthesized hydroxylated azine-based COFs (RIO-11, RIO-11m, RIO-12, RIO-13) *via* the condensation of hydrazine hydrate with 1,3,5-triformylbenzene. Their study focused on understanding the structure–property relationships governing CO_2 adsorption by correlating surface chemistry and textural features with gas uptake performance.[88]

Targeted functionalization continues to drive advances in COF design. In 2022, M. Yin *et al.* fabricated imine-linked triazine COFs functionalized with amino-terminated ionic liquids. These modified materials demonstrated enhanced CO_2 capture due to strong electrostatic, acid–base, and van der Waals interactions between CO_2 and the functional groups. Additionally, the nucleophilic halide groups in the ionic liquids facilitated chemical conversion of captured CO_2, indi-

cating dual functionality.[89] In 2023, Y. He *et al.* developed pyrazine-based COFs (TFPPz-MPA-COF and TFPPz-BD(OMe)$_2$-COF) through the condensation of tetra(4-formylphenyl)pyrazine with respective diamines. These frameworks exhibited significant potential for both CO_2 and iodine adsorption, providing a versatile platform for multifunctional separation applications.[90] Olefin-linked COFs have recently emerged as highly promising materials for direct air capture due to their exceptional chemical stability, high CO_2 capacity, and adaptability for functionalization. Recently, Z. Zhou *et al.* reported the synthesis of COF-999-N_3, an olefin-linked precursor COF that was further modified through reduction and aziridine functionalization to yield COF-999. Outdoor testing in Berkeley, California over 100 adsorption–desorption cycles demonstrated complete retention of performance, underscoring the robustness of these frameworks.[91]

Additionally, linkage engineering presents a novel route to enhance COF performance H. Chen *et al.* developed a method to convert imine-linked COFs into amide-linked frameworks. The imine-PA-TAT COF, synthesized from 4,4′,4″-(1,3,5-triazine-2,4,6-triyl)trianiline and 1,4-phthalaldehyde, was oxidized to form amide-PA-TAT. Mechanistic studies revealed that the carbonyl groups in amide linkages create strong electrostatic fields, resulting in a fourfold increase in CO_2 adsorption relative to imine linkages due to stronger interaction with the CO_2 molecule.[92] Collectively, these studies demonstrate the rapid evolution of imine-linked and functionalized COFs as viable materials for CO_2 capture. Through structural innovation, functional group incorporation, and linkage transformation, COFs continue to expand their role as high-performance adsorbents in gas separation technologies.

3. Architectural design

Adsorption is a key process for CO_2 capture and plays a significant role in many emerging technologies aimed at reducing carbon emissions. This process involves the adsorption of carbon dioxide molecules onto adsorbent surfaces through weak, non-covalent interactions, including van der Waals forces and electrostatic interactions between the quadrupole moment of CO_2 and the dipole moments within the porous frameworks.[93,94] There are various adsorption-based methods for CO_2 capture, with material selection and techniques being influenced by factors such as cost, effectiveness, and specific application requirements.[95] Adsorption can either be physical (physisorption) or chemical (chemisorption), depending on the nature of the interactions between CO_2 and the adsorbent, illustrated in Fig. 5. Carbon dioxide adsorption using physical adsorbents is driven by weak van der Waals and electrostatic

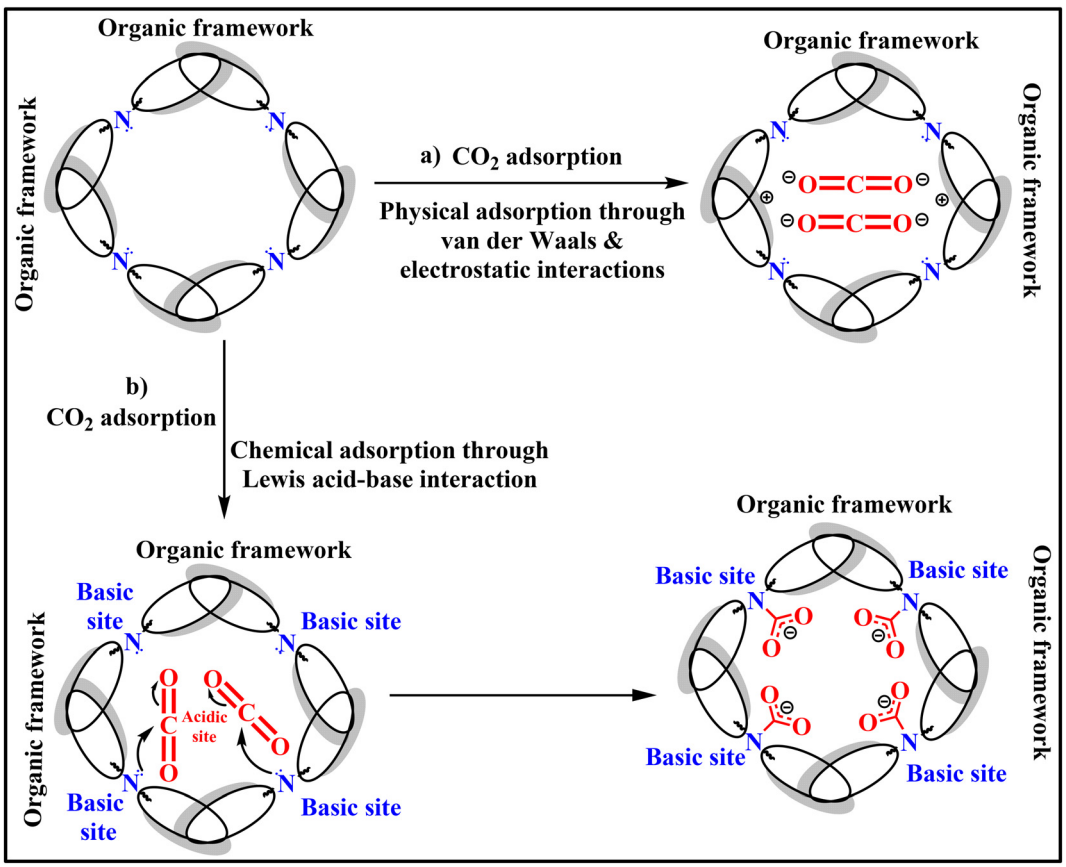

Fig. 5 Schematic representation of the mechanisms involved (a) physical adsorption and (b) chemical adsorption in CO_2 capture.

interactions, which require less energy compared to chemical adsorbents.[96] This is because no new bonds are formed between CO_2 and the adsorbent surface, leading to a lower energy penalty during CO_2 regeneration. The reaction mechanism in chemical adsorption is driven by the Lewis acid–base interaction between CO_2 and nitrogen-rich groups, where the nitrogen-rich group acts as a base and CO_2 as an acidic gas, creating a strong attraction between the two.[97] On the other hand, chemical adsorption involves the formation of stronger bonds between CO_2 and the adsorbent, resulting in a higher CO_2 uptake capacity compared to physical adsorption. This makes chemical adsorption especially useful in post-combustion capture, pre-combustion capture, and direct air capture (DAC) technologies.[98] While physical adsorption of CO_2 on COFs is considered more energy-efficient due to the ease of desorption, chemisorption offers significant benefits in enhancing adsorption capacity, particularly at low pressures.[98]

Both mechanisms are governed by the diffusion of CO_2 into porous structures with pores tailored to CO_2 size, followed by interaction and, ultimately, reversible CO_2 release, contingent on the external conditions.[99] To effectively capture and separate CO_2 from air or flue gas streams using nanoporous adsorbents, it is crucial to account for the impact of humidity. H. Veldhuizen *et al.* explored the effectiveness of a polyimide COF (TAPB-NDA-COF) for CO_2 separation from humid CO_2/N_2 streams, given that water vapour, common in flue gas, can significantly reduce the adsorbent's efficiency by competing with CO_2 for adsorption sites.[100] The TAPB-NDA-COF, which has substantial supermicropore and mesopore volumes, appears advantageous for enhancing water-assisted CO_2 adsorption. Additionally, the abundance of aromatic planes in the COF may facilitate the formation of aromatic motifs that preferentially adsorb CO_2 over water.[101] Moreover, the kinetic diameter of CO_2 is approximately 3.30 Å (0.33 nm), closely comparable to that of N_2, which is 3.64 Å (0.36 nm).[102] This similarity in molecular size highlights the importance of selective sorbent design for effective CO_2 separation, which is influenced by both textural and geometric properties. Key textural properties include thermal conductivity and heat capacity, while geometric considerations involve pore architecture and material morphology.[103] An essential thermodynamic parameter for evaluating adsorbents is the isosteric heat of adsorption (Q_{st}). For optimal CO_2 capture performance, Q_{st} should ideally fall within the range of −20 to −50 kJ mol^{-1}, balancing adsorption strength and energy efficiency. Values more negative than −50 kJ mol^{-1} suggest chemisorption, while less negative values typically indicate physisorption-dominated interactions.[104] In a notable study, N. Huang *et al.* synthesized positively charged imine-linked COFs incorporating 6-bis(4-formylbenzyl)-1,3-dimethyl-benzimidazolium bromide (BFBIm) as a cationic building unit and 4,4′,4″,4‴-(pyrene-1,3,6,8-tetrayl)tetraaniline (PyTTA) as a neutral node. The resulting PyTTA-BFBIm-iCOF exhibited an excellent CO_2 uptake capacity of 177 mg g^{-1} at 273 K and 1 bar, with a Q_{st} of −30.2 kJ mol^{-1}, indicating efficient physisorptive interaction.[105] C. Ji *et al.* reported the synthesis of 3D cage-based COFs utilizing a linear ditopic ligand as a 2-connected linker and an amino-functionalized D_3h-symmetric organic cage as a 6-connected node. Structural distortion and the presence of polar functional groups led to variations in aperture sizes; however, all resulting 3D-OC-COFs demonstrated high thermal and chemical stability along with permanent porosity. Among these, 3D-OC-COF-OH displayed a CO_2 uptake of 174.83 mg g^{-1} and a Q_{st} of 22.4 kJ mol^{-1} under standard conditions (273 K, 1 bar).[106] Thermal conductivity in porous materials is inversely related to pore size, as increased porosity introduces more voids filled with air or vacuum, reducing the material's ability to conduct heat.[107] Furthermore, the development of polymeric frameworks with ultra-micropores (<0.7 nm) has been shown to enhance CO_2 capture, with microporosity contributing linearly to total pore volume and, consequently, gas uptake capacity.[108]

In the context of COF design, the selection of topologies, linkages, and monomer geometries plays a fundamental role in defining the material's structural and functional properties. Nanoarchitectonics, the design and manipulation of materials at the nanoscale to achieve specific structural and functional outcomes, plays a pivotal role in optimizing these parameters.[109] In COFs, nanoarchitectonics refers to the assembly of nanoscale components such as organic linkers, functional groups, *etc.*, into ordered porous crystalline structures with customized properties suited for applications like gas storage, catalysis and sensing.[110] Monomer symmetries – such as C_1, C_2, C_3, C_4, C_6, and T_d – are predictive of the resulting COF topology, which directly impacts CO_2 capture efficiency. For example, T. Banerjee *et al.* synthesized a series of imine-linked [4 + 3] 2D COFs using tetra- and tritopic linkers, achieving a **bex** net topology and a CO_2 uptake of 127 mg g^{-1} at 273 K and 1 bar.[111] Y. Meng *et al.* developed porphyrin-based COFs from [C_4 + C_2] symmetric linkers for 2D structures, and from C_4 and T_d symmetric monomers for 3D frameworks with **pts** topology. The resulting 3D **pts** COFs displayed significantly higher CO_2 uptake (205 mg g^{-1} at 273 K and 1 bar), approximately 3.1 times greater than their 2D counterparts, owing to their narrower pore size distribution, higher free volume, and reduced density.[112] Other notable examples of 3D COFs include an azine-linked framework with a **dia** topology that showed a CO_2 uptake of 123.1 mg g^{-1} under the same conditions.[86] Additional topologies reported for imine-linked COFs with promising CO_2 capture performance include **ljh**,[113] **lon**[114] (featuring 4-connected nodes); **tbo**,[115] **fjh**,[116] **stp**,[117] **hea**,[118] and **she**[119] (based on 6-connected nodes); and **scu**,[120] **flu**[121] (with 8-connected nodes). These studies collectively demonstrate that the precise engineering of COF topology, monomer symmetry, and pore architecture can significantly enhance their applicability for selective and efficient CO_2 capture.

4. Structural linkages in COFs

The term "linkage" in covalent organic frameworks refers to the specific covalent bonds that connect organic building

blocks (monomers) within their two- or three-dimensional architectures. These linkages are central to the exceptional versatility of COFs, as they allow for the precise modulation of properties such as porosity, thermal and chemical stability, electrical conductivity, and catalytic functionality.[85] The selection of linkage chemistry in covalent organic frameworks is primarily guided by the target application, which may include gas storage and separation, catalysis, or energy storage. A diverse range of covalent linkages has been explored in COF synthesis, including C–C, C–N, B–N, B–O, C–S, C=N (*e.g.*, imine), and P–O/P–N linkages. The chemical nature of these linkages significantly influences the framework's stability, porosity, and interaction with guest molecules. H. Furukawa *et al.* investigated the CO_2 adsorption capacities of COF-1 and COF-102, both featuring a boroxine linkage, at low (1 bar) and high pressures (35 and 55 bar), finding that at 273 K and 1 bar, COF-1 and COF-102 exhibited CO_2 uptakes of approximately 98 mg g^{-1} and 68.6 mg g^{-1}, respectively.[65] Z. Kahveci *et al.* synthesized a 2D mesoporous COF called TDCOF-5, formed from 1,4-benzenediboronic acid and hexahydroxytriptycene, which demonstrated a CO_2 uptake of 92.12 mg g^{-1} at 273 K and 1 bar.[122] However, C. Jia *et al.* reported the CO_2 uptake capacities of COF-1[45,123] and tetraethylenepentaamine (TEPA)-modified COFs, TEPA(*n*)COF-1 having boroxine linkage, with $n = 5$ and $n = 10$, which were 78.79, 97.61, and 105.84 mg g^{-1}, respectively. The modification of COF-1 with oligoamine (TEPA) introduces additional interaction sites for CO_2, owing to the abundance of amine groups, resulting in a significant increase in CO_2 adsorption.[118] Nitrogen-rich groups provide active sites that enhance CO_2 adsorption by promoting interactions through electrostatic forces and hydrogen bonding, distinguishing them from other linkages, such as boron-containing groups, in COF materials designed for CO_2 capture.

B. P. Biswal *et al.* developed a β-ketoenamine-linked COF (TpBD) *via* a [3 + 2] reaction between 1,3,5-triformylphloroglucinol (Tp) and benzidine (BD), which demonstrated a CO_2 adsorption capacity of 85 mg g^{-1} at 273 K.[124] Building on this, S. Chandra *et al.* synthesized modified β-ketoenamine-linked COFs incorporating various electron-donating and electron-withdrawing groups to improve CO_2 capture. Among these, nitro-substituted COFs [TpBD-NO_2 and TpBD-$(NO_2)_2$] showed enhanced CO_2 uptake capacities of 124 and 103 mg g^{-1} at 273 K, respectively. In contrast, the fluoro-substituted COF (TpBD-F_4) showed a lower uptake of 69 mg g^{-1} COFs modified with methyl and methoxy groups [TpBD-Me_2 and TpBD-$(OMe)_2$] had CO_2 adsorption capacities of 73 and 53 mg g^{-1}, respectively, at the same temperature.[125] A. F. El-Mahdy *et al.* synthesized β-ketoenamine-linked COFs (TFP-TPA, TFP-Car, TFP-TPP) *via* a one-pot [3 + 3] polycondensation reaction between 1,3,5-triformylphloroglucinol and tris(aminophenyl) derivatives, and they achieved higher CO_2 uptakes of 183, 190, and 200 mg g^{-1}, respectively, at 273 K and 1 bar.[126] D. Kaleeswaran *et al.* synthesized imine and β-ketoenamine tethered COFs by the condensation between 1,3,5-tris (40-aminophenyl)benzene (TAPB) and 1,3,5-tris(40-amino-30,50-isopropylphenyl)benzene (iPrTAPB) with 1,3,5-tris(40-formylphenyl)benzene (TFPB) and 1,3,5-triformylphlurogluconol (TFP) resulting crystalline 2D frameworks, TAPB-TFPB, iPrTAPB-TFPB, TAPB-TFP and iPrTAPB-TFP having CO_2 uptake of 40.1, 31.2, 180, 105.2 mg g^{-1} respectively.[127] β-Ketoenamine linkages provide more effective CO_2 capture than imine linkages due to their stronger CO_2 interactions. However, their

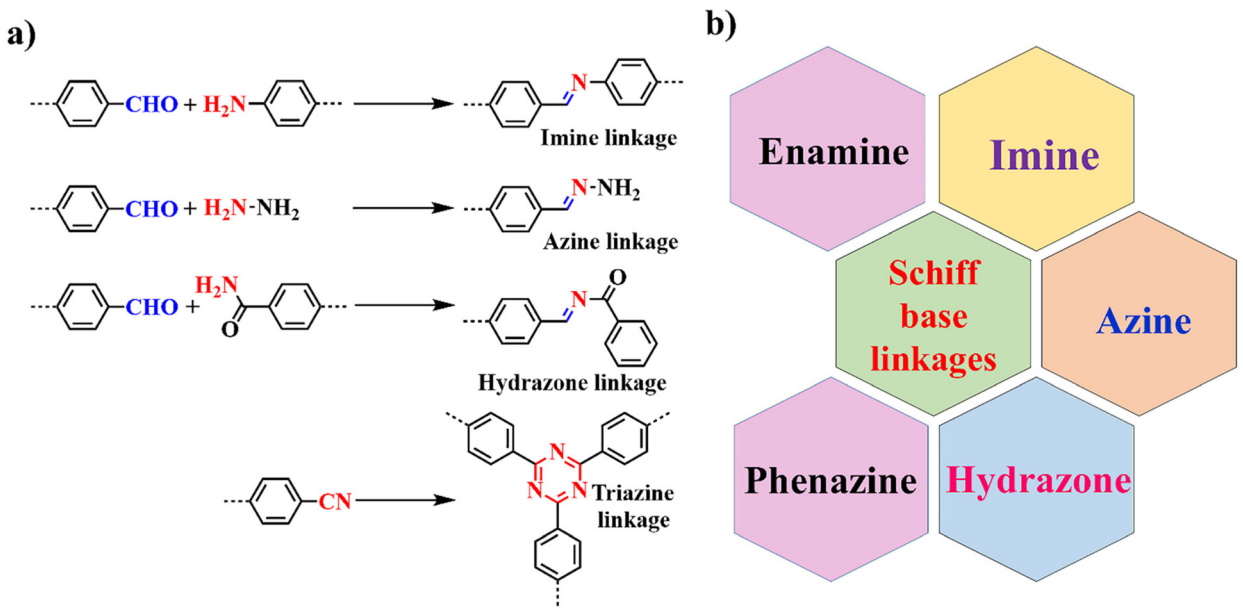

Fig. 6 (a) Schematic representation of –C=N– bonding interactions in COFs discussed in this class of materials. (b) The diagram illustrates the different bonding interactions constructed *via* Schiff base chemistry that contribute to the structure of COFs.

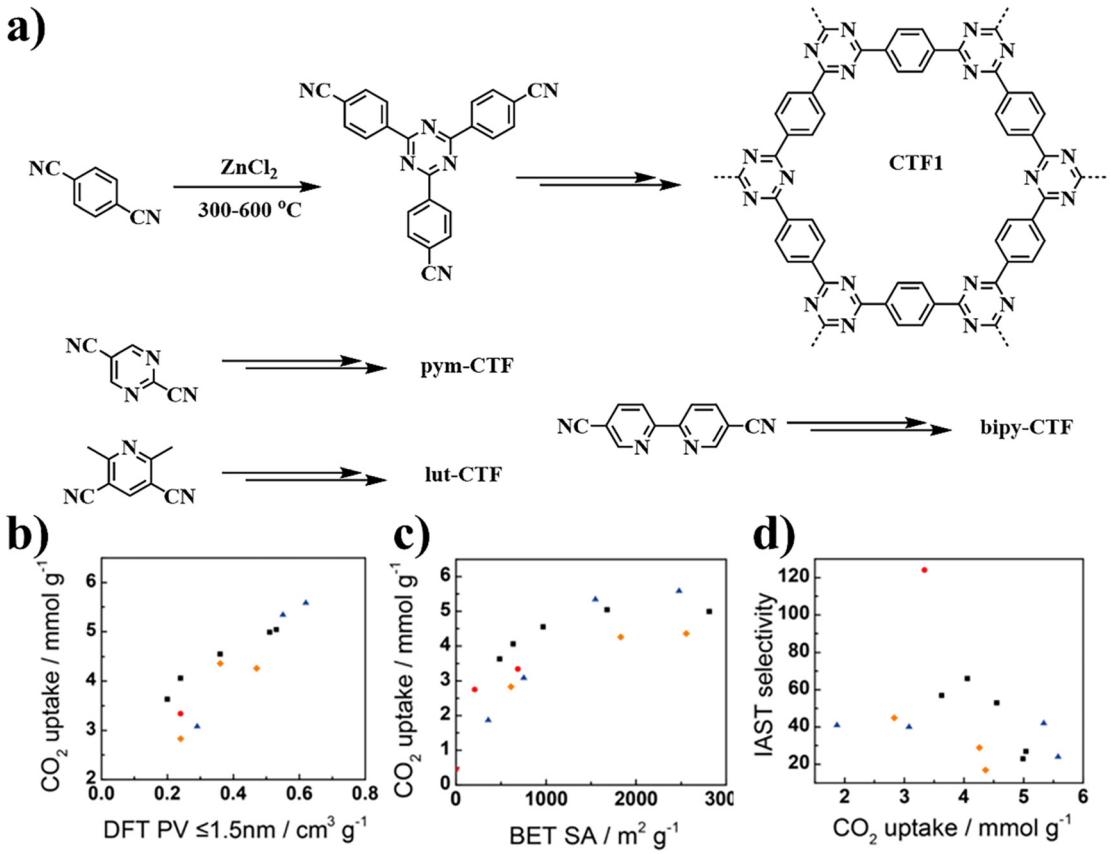

Fig. 7 (a) Synthetic scheme of the CTFs: CTF1, pym-CTF, lut-CTF, and bipy-CTF. (b) CO_2 uptake on the micropore volume (≤1.5 nm). (c) BET SA and (d) IAST selectivity on the CO_2 uptake. lut-CTFs (black squares), pym-CTFs (red circles), bipy-CTFs (blue triangles), and CTF1s (orange diamonds). Reproduced from ref. 129 with permission from the American Chemical Society, Copyright 2015.

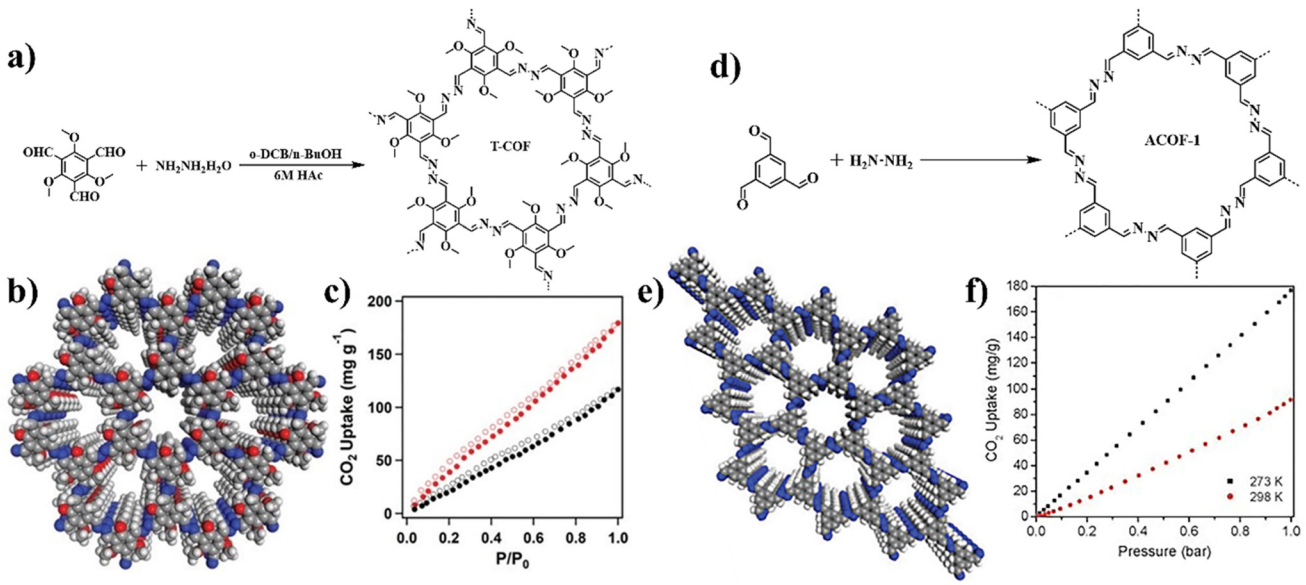

Fig. 8 (a) Schiff base reaction scheme of T-COF. (b) Crystal structure of T-COF with AA stacking model. (c) CO_2 isotherms at 273 K and 298 K of T-COF. Reproduced from ref. 131 with permission from the Royal Society of Chemistry, Copyright 2022. (d) Synthetic scheme of ACOF-1. (e) Top view of AA stacking structure of ACOF-1. (f) CO_2 isotherms of ACOF-1 at 273 K and 298 K. Reproduced from ref. 132 with permission from the Royal Society of Chemistry, Copyright 2014.

synthesis often requires specific monomers and conditions, such as tautomerization, making them less commonly used compared to other C=N linkages.[127]

For CO_2 capture, functionalization of the COF backbone with electron-rich or basic groups such as triazine, imide, tetrazole, and amine moieties has proven particularly effective. These functional groups, due to their high polarizability and strong quadrupole interactions with CO_2, enhance the CO_2-philic nature of the materials. For that, Schiff base chemistry has been widely employed for constructing COFs, especially those involving C=N and C–N linkages. Common examples include imine, azine, and hydrazone linkages,[128] as well as triazine-based frameworks,[124] as illustrated in Fig. 6. Among these, this review places emphasis on COFs containing C–N linkages, owing to the favorable chemical stability and tunable interaction dynamics afforded by the carbon–nitrogen bond network. These features make C=N linked COFs particularly promising candidates for CO_2 capture and related gas separation applications.

S. Hug *et al.* have developed a series of efficient physisorbent materials for gas adsorption and storage using triazine-based frameworks. Covalent Triazine Frameworks (CTFs) were synthesized *via* an isothermal polymerization approach incorporating various functional units such as lutidine, bipyridine, pyrimidine, and phenyl groups shown in Fig. 7. Their findings indicate that while nitrogen content in the CTFs contributes marginally to CO_2 adsorption through weak interactions, the predominant factor responsible for high uptake is the presence of ultramicropores. These pores not only enhance gas sorption by providing high surface area but also increase the accessibility of nitrogen sites, facilitating interactions through Lewis acid–base mechanisms. The CO_2 interaction energy is thus dependent on both the quantity and nature of nitrogen functionalities present in the framework.[129] In a complementary study, J. Du *et al.* reported the synthesis of benzodiimidazole-functionalized CTFs from a dicyano-substituted benzodiimidazole monomer. This material exhibited a notable CO_2 uptake of 89.2 $cm^3\ g^{-1}$ (174.83 mg g^{-1}) at 273 K and 1 bar, with isosteric heats of adsorption reaching up to 52 kJ mol^{-1}, highlighting the combined contributions of microporosity and nitrogen enrichment in enhancing adsorption capacity.[130]

Beyond triazine-based frameworks, Schiff base linkages, particularly azine bonds, have shown considerable promise for CO_2 capture. Y. Zhang *et al.* synthesized an azine-linked covalent organic framework (T-COF) through the condensation of 2,4,6-trimethoxybenzene-1,3,5-tricarbaldehyde and hydrazine demonstrated in Fig. 8a. The T-COF exhibited a high CO_2 uptake of 178 mg g^{-1} at 273 K, attributed to its nitrogen- and

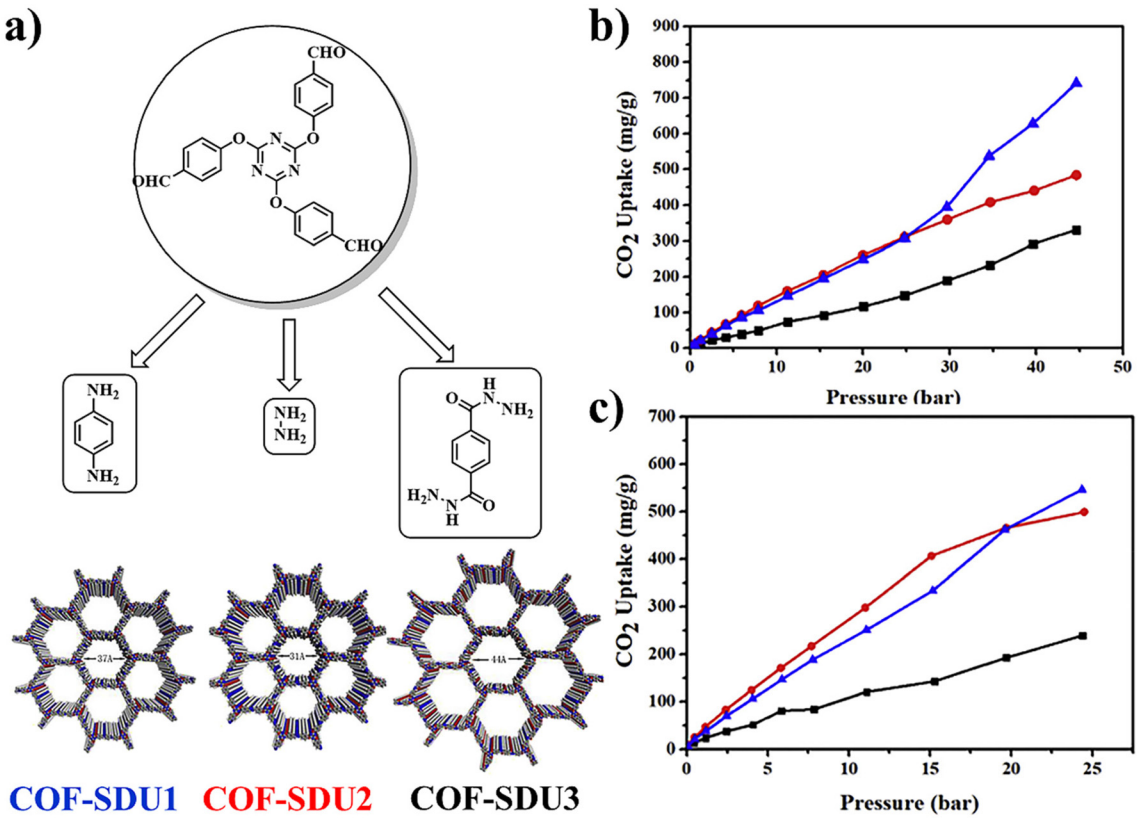

Fig. 9 (a) Illustration of different bonding motifs in COFs with imine, azine, and hydrazone linkages. (b) CO_2 uptake of COFs, COF-SDU1 (blue triangle), COF-SDU2 (red cycle), COF-SDU3 (black square) at 298 K. (c) CO_2 uptake at 273 K. Reproduced from ref. 134 with permission from the Elsevier, Copyright 2019.

oxygen-rich skeleton and uniform pore size of approximately 0.82 nm, as determined by non-local density functional theory (NLDFT). These embedded polar functional units and microporous architecture synergistically promote high CO_2 affinity.[131] Z. Li *et al.* further demonstrated the potential of azine-linked COFs by synthesizing ACOF-1 *via* solvothermal condensation of 1,3,5-triformylbenzene with hydrazine hydrate. ACOF-1 exhibited a high surface area (1318 m^2 g^{-1}) and a CO_2 uptake of 17.7 wt% at 273 K and 1 bar shows in Fig. 8f. The isosteric heat of adsorption (Q_{st}) was measured at 27.6 kJ mol^{-1}, surpassing that of many previously reported imine-linked COFs, organic cages, and diimide polymers. The enhanced gas uptake is attributed to the interplay between high surface area, optimal pore size, and the availability of nitrogen sites.[132]

Hydrazone-linked COFs also present attractive characteristics for CO_2 capture, owing to their high nitrogen content, structural tunability, synthetic versatility, and robust thermal and chemical stability. N. Bagherian *et al.* synthesized a hydrazone-linked COF (TPT/OH COF) *via* solvothermal condensation of oxalyl dihydrazide and 2,4,6-tris(*p*-formylphenoxy)-1,3,5-triazine (TPT) illustrated in Fig. 9. This framework demonstrated a CO_2 uptake of 0.9 mmol g^{-1}, attributed to its extended π-conjugation, nitrogen-rich pore walls, high surface area, narrow pore size, and stable hydrazone linkages.[133] Additionally, M. Zhang *et al.* constructed three COFs using tri-(4-formylphenoxy)-1,3,5-triazine (TRIF) and various linkers, including *p*-phenylenediamine (imine linkage), hydrazine (azine linkage), and terephthalic dihydrazide (hydrazone linkage). Their study revealed that larger pore sizes favoured CO_2 uptake under high-pressure conditions (>25 bar), whereas BET surface area was the dominant factor under low-pressure conditions (<25 bar). Among the three, COF-SDU1 exhibited the highest CO_2 uptake (compared in Table 4), which was attributed to its high surface area, large pore volume, and the presence of both triazine rings and imine functionalities.[134] Imine-linked COFs offer the benefits of high surface area and easy modifiability, making them ideal

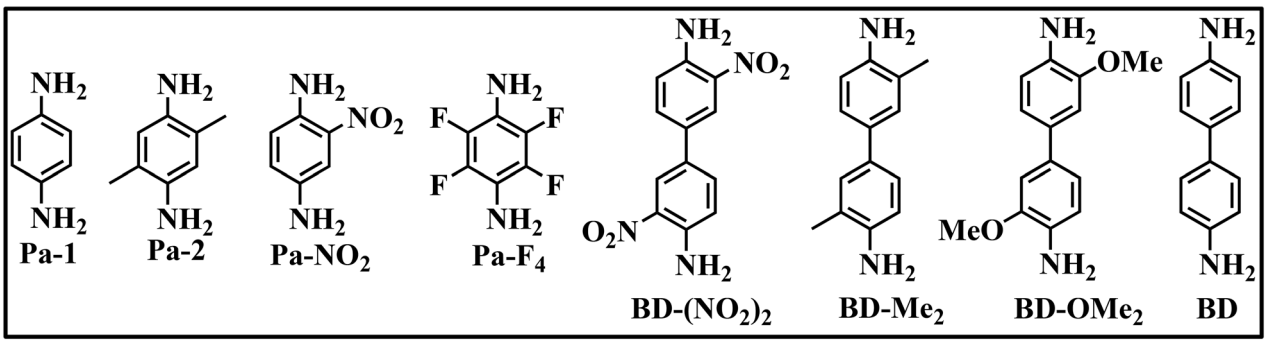

Fig. 10 Different functionalized amino monomers utilized by Chandra *et al.* for the condensation with 1,3,5-triformylphloroglucinol (Tp).[125]

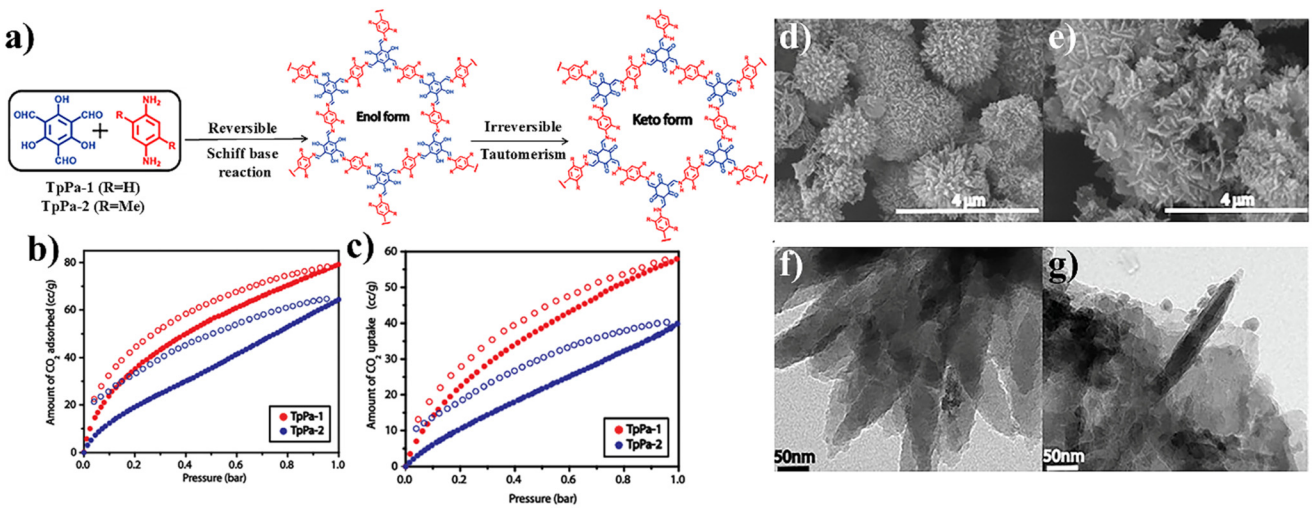

Fig. 11 (a) Synthetic scheme of the COFs, TpPa-1 & TpPa-2. (b) CO_2 uptake of TpPa-1 & TpPa-2 at 273 K. (c) CO_2 uptake of TpPa-1 & TpPa-2 at 298 K. (d and e) TEM images of TpPa-1. (f and g) TEM images of TpPa-2. Reproduced from ref. 141 with permission from the American Chemical Society, Copyright 2012.

for optimizing CO_2 adsorption by post-synthetic functionalization.

5. Schiff base imine linkage

Among the various linkages developed to date, imine linkages have emerged as particularly significant for applications in carbon dioxide (CO_2) capture and sequestration. This prominence is due to their synthetic accessibility, reversible formation *via* Schiff base condensation, tunable reactivity, and ability to support microporosity while accommodating diverse topologies. Generally, they demonstrate significant stability in a wide range of organic solvents and exhibit minimal sensitivity to aqueous conditions, as well as both acidic and basic environments.[135] Schiff base imine-linked COFs often rely on amines and aldehydes, which are relatively inexpensive but require high purity for high-performance frameworks.[136] An initial advancement in this area was reported by F. J. Uribe-Romo *et al.* in 2009, with the synthesis of COF-300, a three-dimensional COF featuring a five-fold interpenetrated diamondoid topology. This framework was constructed *via* the reversible condensation of aldehydes and amines to form imine bonds, demonstrating the combined application of reticular chemistry and dynamic covalent chemistry to produce structurally ordered and functionally robust materials.[137] Also, the ability to scale up and the cost-efficiency of Schiff base imine-linked COFs are the crucial factors that will determine their feasibility for large-scale industrial applications in CO_2 capture.[136] The synthesis of Schiff base imine-linked COFs often relies on solvent-based condensation (solvothermal method) reactions between amines and aldehydes, which can be challenging to scale efficiently. The combination of mesitylene, dioxane, and acetic acid (AcOH) is commonly used as the most effective solvent mixture.[138] Other solvent systems, such as dioxane-aqueous acetic acid and *n*-butanol (*n*-BuOH)/*o*-dichlorobenzene (*o*-DCB)/3 M AcOH, have also been widely employed. AcOH, typically serving as the catalyst, plays a critical role in the formation of the imine linkage.[139] Alternatively, microwave synthesis and mechanochemical (MC) synthesis are widely explored in the synthesis of imine-based COFs.[136] B. P. Biswal *et al.* were the pioneers in employing mechanochemical techniques to efficiently synthesize two chemically stable COFs (TpPa-1 and TpPa-2) using a mortar and pestle system at room temperature. These COFs, synthesized *via* solvent-free mechanochemical methods, demonstrated moderate crystallinity, impressive stability, and high scalability.[124] Subsequently, H. Wei *et al.* employed a microwave-assisted solvothermal method to synthesize the 2D imine-linked COF (TpPa-COF) *via* a Schiff base reaction between 1,3,5-triformylphloroglucinol and *p*-phenylene diamine, achieving a higher yield in less time and TpPa-COF (MW) showing CO_2 uptake of 224.4 mg g^{-1} at 273 K and 1 bar.[140] These methods eliminate the need for toxic solvents and facilitate large-scale production, potentially making them suitable for industrial applications. The scalability of imine-based COFs is also tied to the cost of synthesis. The economic viability of scaling up production will rely on factors such as the availability of affordable monomers, the chosen synthesis methods, and the energy demands associated with large-scale manufacturing.

5.1. Tunable Schiff base imine linkages in COFs: functionalization

The initial study of carbon dioxide (CO_2) adsorption by imine-linked covalent organic frameworks was reported in 2012 by

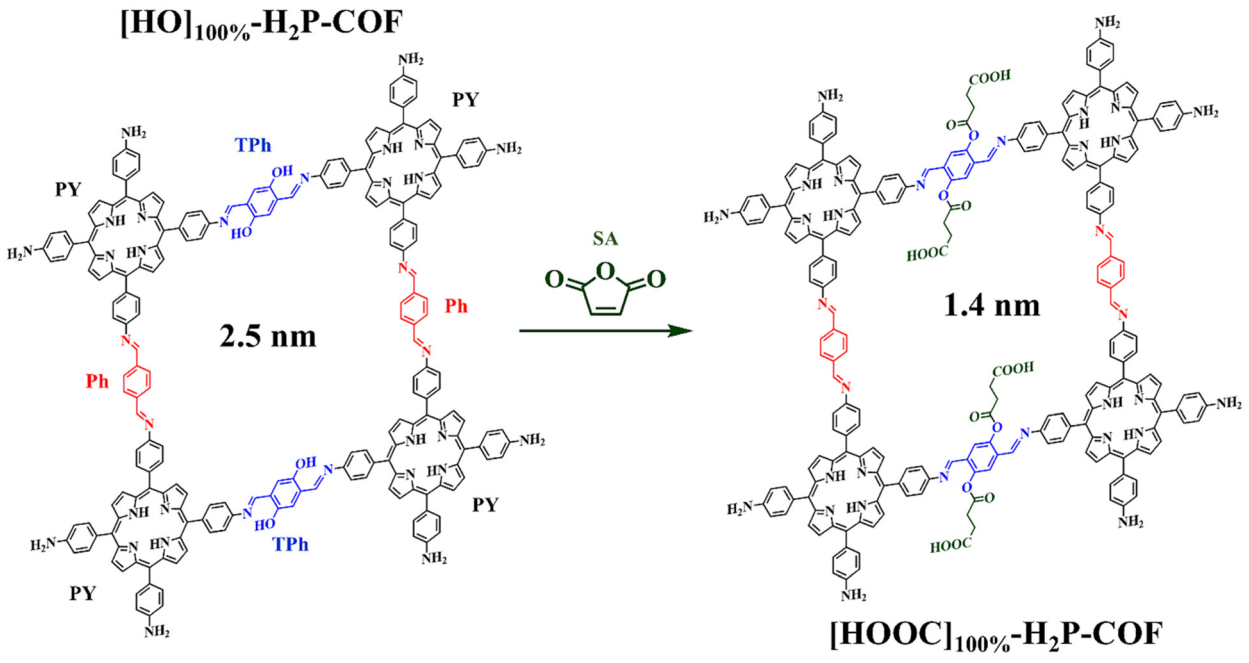

Fig. 12 Structural representation of $[HO]_{100\%}$-H_2P-COF and $[HOOC]_{100\%}$-H_2P-COF.[142]

S. Kandambeth *et al.*, who synthesized two chemically robust two-dimensional COFs, TpPa-1 and TpPa-2, *via* reversible and irreversible Schiff base solvothermal reactions. These frameworks were obtained through the condensation of 1,3,5-triformylphloroglucinol (Tp) with *p*-phenylenediamine (Pa-1) and 2,5-dimethyl-*p*-phenylenediamine (Pa-2), respectively shows in Fig. 11a. The resulting materials exhibited CO_2 uptake capacities of 80 $cm^3\ g^{-1}$ and 63 $cm^3\ g^{-1}$ at 273 K and 1 bar, respectively. Both frameworks underwent irreversible tautomerism from the enol–imine to keto-enamine form, conferring excellent acid (9 N HCl) and thermal stability due to the absence of hydrolyzable imine linkages. Notably, both COFs demonstrated a characteristic flower-like morphology upon crystallization.[141] Subsequently, S. Chandra *et al.* expanded this platform by synthesizing a series of functionalized imine-linked COFs, including TpPa-NO_2, TpPa-F_4, TpBD-$(NO_2)_2$, TpBD-Me_2, TpBD$(OMe)_2$, and TpBD, using various substituted diamine and dialdehyde monomers (Fig. 10). These COFs exhibited pore sizes ranging from 1.5 to 2.4 nm.[125]

However, the densely packed, π-stacked architecture of 2D COFs can restrict their gas adsorption performance due to limited accessible pore volume and surface area. To address this limitation, N. Huang *et al.* (2015) introduced wall-functionalized imine-linked COFs constructed from porphyrin units and phenol-containing aldehydes, facilitating post-synthetic modification of the pore walls with carboxylic acid groups *via* a ring-opening reaction with succinic anhydride (Fig. 12).[142] By modulating the proportion of phenol groups through a three-component condensation strategy, the CO_2-philic functionality was precisely tuned. A 100% carboxylate-functionalized COF demonstrated an enhanced CO_2 uptake of 174 mg g^{-1} at 273 K and 1 bar, despite a concurrent reduction in porosity.[142,143]

The incorporation of triazine moieties into polymer frameworks has been widely reported to enhance their suitability for CO_2 adsorption and sensing applications.[144] In the same year, R. Gomes *et al.* reported TRITER-1, an imine-linked COF prepared *via* a one-pot Schiff base condensation of terephthalaldehyde with 1,3,5-tris(4-aminophenyl)triazine. This work also marked the first example of a superacid-catalyzed trimerization of 4-aminobenzonitrile to form the triazine core.[145] These nitrogen-rich frameworks, characterized by their mesoporous structure (~1.7 nm), large surface area (716 $m^2\ g^{-1}$), and

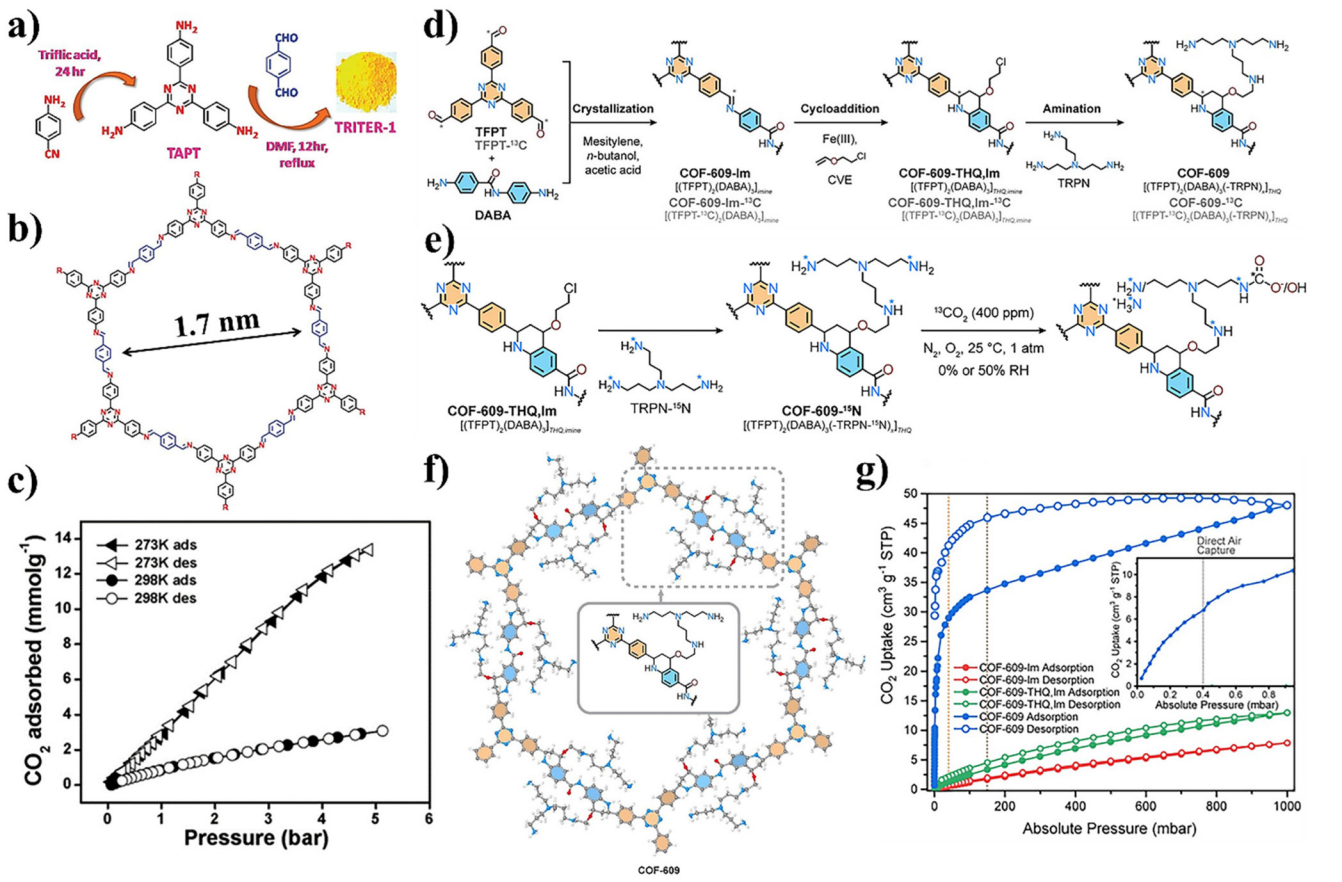

Fig. 13 (a) Schematic outline for the synthesis of COF, TRITER-1. (b) Designed structure of TRITER-1. (c) CO_2 isotherms of TRITER-1 at 273 K and 298 K. Reproduced from ref. 145 with permission from the American Chemical Society, Copyright 2015. (d) Synthetic pathway of COF-609 with labelled C13. (e) COF-609-^{15}N synthetic scheme and its chemisorption with $^{13}CO_2$. (f) Proposed structure of COF-609. (g) CO_2 adsorption and desorption isotherm of COF-609-Im, COF-609-THQ & COF-609. Reproduced from ref. 147 with permission from the American Chemical Society, Copyright 2022.

thermal stability, exhibited exceptional CO_2 adsorption capacities, up to 58.9 wt% at 273 K and 13.7 wt% at 298 K under 5 bar pressure illustrated in Fig. 13(a–c).[145] Similarly, S. Wu *et al.* synthesized imide-functionalized triazine COFs (TPIs@IC) through a two-step process, achieving a CO_2 uptake capacity of 3.2 mmol g^{-1} at 273 K and 1 bar.[146]

In a notable advancement, H. Lyu *et al.* developed aliphatic amine-linked COFs derived from imine precursors *via* a post-synthetic tetrahydroquinoline (THQ) linkage transformation. The resulting framework, COF-609, displayed strong chemisorption characteristics and significantly enhanced CO_2 uptake (6.8 cm^3 g^{-1} or 0.304 mmol g^{-1} at 0.4 mbar), in contrast to its precursor (COF-609 THQ-Im), which exhibited only 0.005 cm^3 g^{-1} (0.00022 mmol g^{-1}) under identical conditions shown in Fig. 13(d–g). This 1360-fold improvement provides compelling evidence that incorporating aliphatic amines into COF structures enables efficient CO_2 capture under ambient conditions, supporting their potential for direct air capture and post-combustion applications.[147]

5.2. Three-dimensional (3D) imine linkages: expanding the dimensionality of COFs

While the majority of covalent organic frameworks reported to date are two-dimensional (2D) layered materials featuring one-dimensional (1D) pore channels, the development of three-dimensional (3D) COFs has attracted growing interest due to their enhanced porosity and potential for gas adsorption.[84] These 2D structures typically rely on non-covalent interactions for layer stacking, whereas 3D COFs offer interconnected networks that may improve guest molecule accessibility and framework stability. Z. Li *et al.* successfully synthesized a 3D COF, termed 3D-ceq-COF, *via* solvothermal condensation between 1,3,5-tris(4-aminophenyl)triazine (TAPT) and 2,3,6,7,14,15-hexakis(4-formylphenyl)triptycene (HFPTP).[148] The incorporation of the triptycene scaffold facilitated the formation of a **ceq** topology and enhanced the exposure of aromatic units, promoting stronger interactions with CO_2 molecules. This framework demonstrated a CO_2 uptake of 179 mg

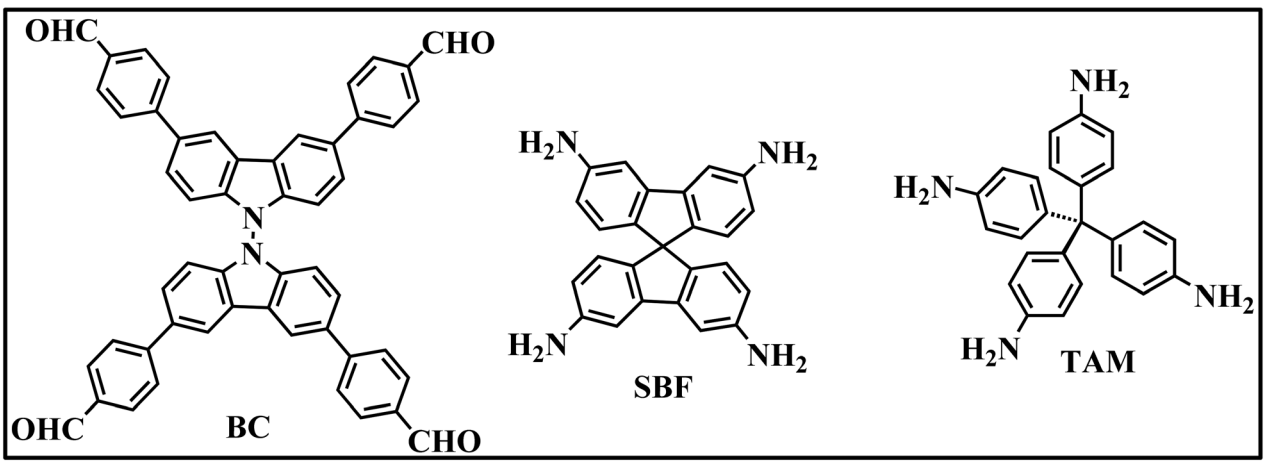

Fig. 14 Representative monomeric scaffolds utilized for the 3D polymeric architectures.

Table 3 Comparison of 2D and 3D COFs: advantages and limitations in CO_2 capture performance, stability, and synthesis complexity

Properties	3D-COFs	2D-COFs
Surface area and porosity	Higher surface area and porosity.	2D COFs have a smaller surface area than 3D COFs.
Stability	It offers superior stability, particularly in terms of thermal and chemical resistance, due to its interconnected framework.	2D COFs have less stability compared to 3D COFs due to their layered structure, which can delaminate under harsh conditions.
CO_2 adsorption capacity	Well-defined and stable pores for selective CO_2 capture.	Lower CO_2 adsorption due to a less rigid structure.
Scalability	Difficult to scale up due to the limited availability of topology design strategies and building blocks.	Constructing layered structures in 2D COFs is challenging, but both diverse building blocks and topology designs provide potential solutions.
Cost	More expensive due to the need for precise monomer design and complex synthesis, which often involves advanced techniques like self-assembly or template-directed methods, adding to the overall cost.	Typically less expensive due to simpler synthesis and diverse building blocks, but costs can rise with scaling and maintaining uniformity.

Table 4 Reported characteristics and CO_2 capture performance of reviewed COF materials

COF materials [Ref.]	Linkage	Surface area ($m^2\ g^{-1}$)	Pore size (nm)	Thermal stability	Chemical stability	CO_2 uptake at 273 K & 1 bar ($mg\ g^{-1}$)	CO_2 uptake at 298 K & 1 bar ($mg\ g^{-1}$)
PyTTA-BFBIm-iCOF[105]	Imine	1532	2.3	450 °C	Stable in water, DMF, HCl (3 M) and NaOH (3 M) for 1 day.	177	93
3D-OC-COF-OH[106]	Imine	923	0.65	430 °C	Stable in organic solvents and water.	174.83	100.94
PY_2B-COFs[104]	Imine	1984	1.83, 2.37	—	Unstable in HCl (1 M) and NaOH (1 M).	127	—
3D-PdPor-COF[104]	Imine	1406	0.58	500 °C	—	205.8	93.49
COF-1[65]	Boroxine	750	0.9	500 °C	—	98	230 (55 bar)
COF-102[65]	Boroxine	3620	1.2	400 °C		68.6	1200 (55 bar)
TDCOF-5[122]	Boroxine	2497	2.6	420 °C		92.12	
TpPa-1[141]	Imine	535	1.25	350 °C	Stable in water and HCl (9 M) for 7 days.	152.88	—
TpPa-2[141]	Imine	339	1.35	350 °C	Stable in water, HCl (9 M) and NaOH (9 M) for 7 days.	125.44	—
CTF1[129]	Triazine	2557	—	—	—	191.84	97.24
pym-CTF[129]	Triazine	689	—	—	—	146.96	94.6
lut-CTF[129]	Triazine	2815	—	—	—	219.56	110.88
bipy-CTF[129]	Triazine	2479	—	—	—	245.52	129.8
T-COF[131]	Azine	587	0.82	350 °C	Stable in water, DMF, HCl (1 M) and NaOH (1 M) for 12 hours.	178	117
ACOF-1[132]	Azine	1318	0.94	300 °C	—	177	~92
TPT/OH COF[133]	Hydrazone	424	3.35	~300 °C	Stable in organic solvents and HCl (9 M) for 1 day.	—	39.6
COF-SDU1[134]	Imine	1008	3.70	400 °C	—	547[a]	741[a]
COF-SDU2[134]	Azine	1070	2.96	350 °C	—	484[a]	500[a]
COF-SDU3[134]	Hydrazone	419	4.30	350 °C	—	331[a]	239[a]
$[HO_2C]_{100\%}$-H_2P-COFs[142]	Imine	364	1.4	~300 °C	—	174	76
TRITER-1[145]	Imine	716	1.7	400 °C	—	588.72[b]	136.84[b]
TPIs@IC[146]	Imide	1053	0.54, 1.48	450 °C	Stable in organic solvents and dil. HCl (10 wt%) for 2 days.	141.68	92.84
3D-ceq-COF[148]	Imine	1148.6	—	550 °C	Stable in organic solvents and water for 1 day.	179	—
3D CageCOF-1[149]	Imine	1040	—	400 °C	Stable in organic solvents and water for 1 day.	204	107
SP-CA-COF-IM[151]	Imine	1551	0.95	~400 °C		110	48.4
SP-CA-COF-AM[151]	Amine	1557	0.95	~400 °C		162.8	80.52
COF-300-SO_3H[153]	Imine	428.42	—	—	—	—	274.12

[a] CO_2 uptake of COF-SDU1, COF-SDU2, and COF-SDU3 was measured at 273 K and 298 K under 45 bar and 25 bar pressures, respectively. [b] CO_2 uptake of TRITER-1 was measured at 273 K and 298 K under 5 bar pressure.

g^{-1} at 273 K and 1 bar, highlighting the role of π–π interactions and molecular recognition sites in enhancing CO_2 adsorption. Despite this progress, expanding the library of 3D COFs remains challenging due to the scarcity of suitable 3D organic building blocks and the limited reversibility of the covalent bonds used in framework construction. Addressing this, Cooper *et al.* developed a 3D organic cage-based COF (3D-CageCOF-1) using a hydrothermal reaction between 4,6,16,18,31,33-hexamino-2,8,14,20,29,35-hexaoxabicyclo[3.3.3] octane-based calixarene (Cage-6-NH_2) and 2,5-dihydroxyterephthalaldehyde (DHTPA).[149] The resulting framework features a microporous environment enriched with oxygen and nitrogen functionalities, forming a polar and hydrophilic cavity ideal for CO_2 adsorption. 3D-CageCOF-1 exhibited an exceptional CO_2 uptake capacity of 204 $mg\ g^{-1}$ under the same conditions.

In a separate study, C. Gao *et al.* synthesized a series of isostructural 3D COFs with **pts** topology *via* [4 + 4] imine condensation using linkers bearing –H, $–CH_3$, or –F substituents.[150] Among these, the F-substituted COF displayed the highest CO_2 uptake, attributed to stronger binding interactions as indicated by a higher isosteric heat of adsorption (Q_{st} = 28.4 $kJ\ mol^{-1}$), despite comparable porosities and pore architectures. L. Zhang *et al.* introduced a rigid, imine-linked 3D COF (SP-CA-COF-IM), synthesized by the condensation of bicarbazole (BC) and spirobifluorene (SBF)-based orthogonal building blocks (Fig. 14).[151] This framework, possessing a dia topology, restricted molecular rotation to produce a structurally brittle lattice. Post-synthetic modification using NaBH$(OAc)_3$ converted the imine linkages into secondary amines, yielding SP-CA-COF-AM. The incorporation of amine functionalities introduced chemisorptive sites, significantly enhancing

the selectivity and capacity for CO_2 capture compared to its imine-linked precursor.

F. Yuan *et al.* employed grand canonical Monte Carlo (GCMC) simulations and density functional theory (DFT) calculations to examine the influence of polar functional groups (–CH_2NH_2, –COOH, –SO_3H) on CO_2 uptake in 3D COFs.[152] Functionalization led to elevated binding energies (19.4–35.1 kJ mol^{-1}) compared to the unfunctionalized frameworks (19.2 kJ mol^{-1}), thereby promoting improved adsorption performance. Similarly, S. Wei *et al.* synthesized a series of functionalized derivatives of COF-300-THF, derived from tetrakis(4-aminophenyl)methane (TAM) and terephthalaldehyde (BDA), modified with –OH, –NO_2, –SO_3H, and –NH_2 groups.[153] The CO_2 adsorption capacity at 298 K and 1 bar progressively increased from 57.2 mg g^{-1} for COF-300-THF to 82.28 mg g^{-1} (COF-300-NH_2), 91.08 mg g^{-1} (COF-300-OH), 187 mg g^{-1} (COF-300-NO_2), and peaked at 274.12 mg g^{-1} for COF-300-SO_3H. These enhancements are attributed to stronger guest–host interactions facilitated by the introduced polar groups and the accompanying reduction in pore size. 3D COFs offer superior stability and higher adsorption capacity, making them ideal for demanding industrial applications.[154] However, they are more complex to synthesize and come at a higher cost. In contrast, 2D COFs are easier to synthesize and more cost-effective, but their lower stability and fragility can limit their long-term effectiveness in CO_2 capture and under harsh conditions, as illustrated in Table 3.[139] Table 4 summarizes the carbon dioxide uptake capacities of various COFs featuring –C–N– linkages, as discussed in this review.

6. Future outlook and conclusions

The Paris Agreement, a landmark global accord ratified by over 190 nations, aims to mitigate climate change by limiting the rise in global average temperatures to well below 2 °C above pre-industrial levels, with efforts directed toward a 1.5 °C threshold. Despite this widespread commitment, current global emissions trajectories remain misaligned with these temperature targets, underscoring the urgent need for advanced carbon capture technologies. In this context, covalent organic frameworks (COFs) have emerged as promising candidates due to their structural tunability, permanent porosity, and functional modularity. To meet both performance and scalability demands, it is imperative to develop adsorbent materials with superior CO_2 capture capabilities. The design of imine-linked 3D COFs represents a significant advancement in the field, effectively combining the chemical robustness and design flexibility of extended frameworks with the synthetic modularity of organic chemistry. However, several critical challenges remain that must be addressed to realize the full potential of these materials.

(1) The targeted construction of ultra-microporous 3D COFs – defined by pore sizes less than 0.7 nm – should be emphasized for their ability to enable high-density CO_2 packing, especially under elevated pressure conditions (>25 bar), aligning with industrial operational demands.[155]

(2) There is a pressing need to explore Schiff base-derived 3D topologies that incorporate CO_2-philic moieties such as nitrogen-rich triazine and polar functional groups like –NH_2, COOH, OH, SO_3H. Modifying the electron density or steric hindrance at these linkage sites can tune the material's ability to

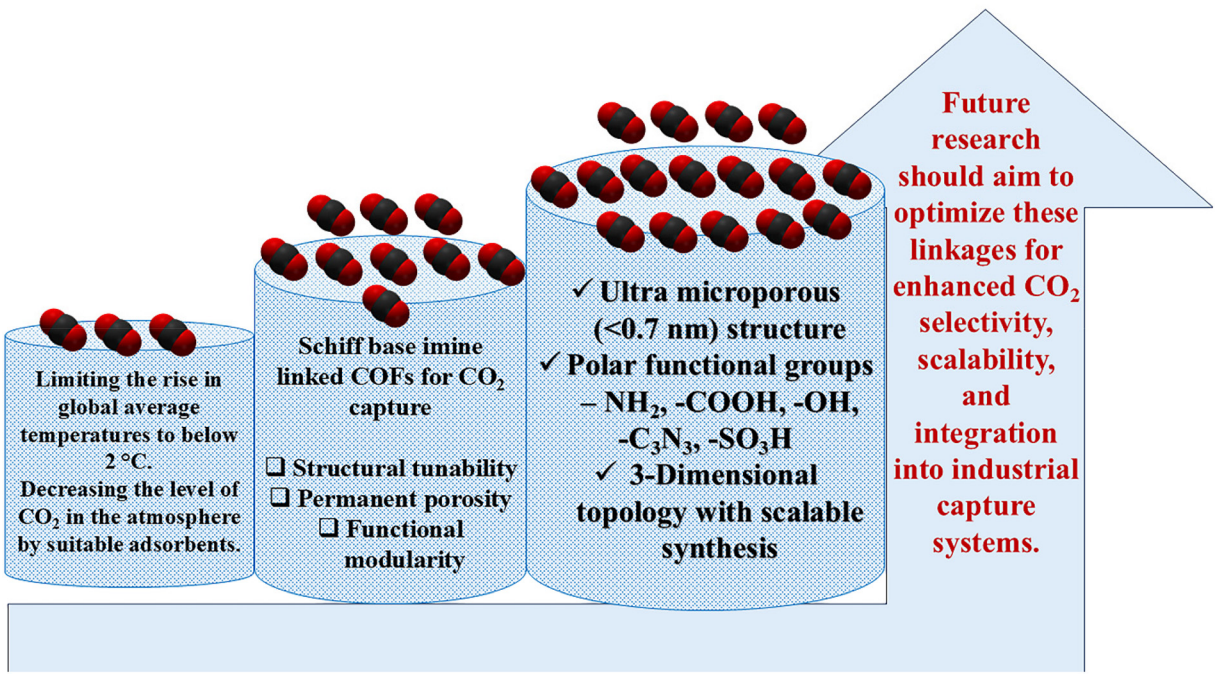

Fig. 15 Schematic diagram summarizing the challenges and solutions for effective CO_2 capture with emphasis on Schiff base imine-linked COFs.

selectively adsorb CO_2. These functionalities could enhance host–guest interactions through Lewis acid–base interactions and significantly improve CO_2 capture ability.

(3) Introducing non-covalent interactions strategies – such as dipole–dipole interactions, van der Waals forces (hydrogen bonding), and electrostatic attractions – offers a promising route to modulate the physicochemical characteristics of Schiff base imine-linked frameworks while preserving their crystallinity and robustness.

In conclusion, while COFs have already demonstrated utility across a range of sectors, further research is essential to address existing limitations. By integrating these design principles with linkage engineering and scalable synthesis techniques, we can enable the rational development of next-generation COFs optimized for efficient, selective, and regenerable CO_2 capture in industrial environments illustrated in Fig. 15. Furthermore, interdisciplinary collaboration, combining computational modeling with experimental synthesis, will be crucial for translating these laboratory findings into practical, real-world industrial applications. These approaches will be crucial for developing next-generation COF materials with enhanced CO_2 capture performance and long-term environmental sustainability. This mini-review underscores the potential of Schiff base imine-linked 3D COFs as a platform for the rational design of chemically and thermally stable, functional porous materials for greenhouse gas adsorption and beyond.

Conflicts of interest

There are no conflicts to declare.

Data availability

No new data were generated or analyzed as part of this review; all data are available in the appropriate references.

Acknowledgements

P. D. R. and A. R. S. thanks the University of Kerala for the research fellowships.

References

1 Q. Ma, *Science briefs: greenhouse gases: refining the role of carbon dioxide*, NASA GISS, 1998.
2 D. A. Lashof and D. R. Ahuja, *Nature*, 1990, **344**(6266), 529–531, DOI: **10.1038/344529a0**.
3 R. T. Watson, L. G. Meira Filho, E. Sanhueza and A. Janetos, *Clim. Change*, 1992, **92**, 25–46.
4 *Intergovernmental Panel on Climate Change, in Contribution of Working Group I to the Sixth Assessment Report of the Intergovernmental Panel on Climate Change*, Cambridge University Press, 2021, DOI: **10.1017/9781009157896**.
5 G. Myhre, D. Shindell, F.-M. Bréon, W. Collins, J. Fuglestvedt, J. Huang, D. Koch, J.-F. Lamarque, D. Lee, B. Mendoza, T. Nakajima, A. Robock, G. Stephens, T. Takemura and H. Zhang, Anthropogenic and natural radiative forcing, in *Contribution of Working Group I to the Fifth Assessment Report of the Intergovernmental Panel on Climate Change*, ed. T. F. Stocker, D. Qin, G.-K. Plattner, M. Tignor, S. K. Allen, J. Boschung, A. Nauels, Y. Xia, V. Bex and P. M. Midgley, Cambridge University Press, 2013, pp. 659–740.
6 M. Karimi, A. E. Rodrigues and J. A. Silva, *Adv. Bioenergy Microfluid. Appl.*, 2021, 255–274.
7 A. M. Bazzanella and F. Ausfelder, *Technology study: low carbon energy and feedstock for the European Chemical Industry*, 2017.
8 S. E. Tanzer and A. Ramírez, *Energy Environ. Sci.*, 2019, **12**(4), 1210–1218, DOI: **10.1039/C8EE03338B**.
9 R. Lindsey, Climate change: atmospheric carbon dioxide. NOAA, Climate.gov, 2024. **https://www.climate.gov/news-features/understanding-climate/climate-change-atmospheric-carbon-dioxide#**.
10 T. R. Karl and K. E. Trenberth, *Science*, 2003, **302**(5651), 1719–1723, DOI: **10.1126/science.1090228**.
11 S. C. Doney, V. J. Fabry, R. A. Feely and J. A. Kleypas, *Ann. Rev. Mar. Sci.*, 2009, **1**(1), 169–192, DOI: **10.1146/annurev.marine.010908.163834**.
12 M. T. Huang and P. M. Zhai, *Adv. Clim. Change Res.*, 2021, **12**(2), 281–286, DOI: **10.1016/j.accre.2021.03.004**.
13 L. Riboldi, *Assessment of pressure swing adsorption as CO_2 capture technology in coal fired power plants*, 2016..
14 M. Songolzadeh, M. Soleimani, M. T. Ravanchi and R. Songolzadeh, *Sci. World J.*, 2014, **1**, 828131, DOI: **10.1155/2014/828131**.
15 G. Cau, V. Tola, F. Ferrara, A. Porcu and A. Pettinau, *Fuel*, 2018, **214**, 423–435, DOI: **10.1016/j.fuel.2017.10.023**.
16 M. M. Hossain and H. I. de Lasa, *Chem. Eng. Sci.*, 2008, **63**(18), 4433–4451, DOI: **10.1016/j.ces.2008.05.028**.
17 J. Davison and K. Thambimuthu, *Greenhouse Gas Control Technol.*, 2005, **7**, 3–13, DOI: **10.1016/B978-008044704-9/50002-1**.
18 M. Karimi, M. Shirzad, J. A. Silva and A. E. Rodrigues, *Environ. Chem. Lett.*, 2023, **21**(4), 2041–2084, DOI: **10.1007/s10311-023-01589-z**.
19 S. Choi, J. H. Drese and C. W. Jones, *ChemSusChem*, 2009, **2**(9), 796–854, DOI: **10.1002/cssc.200900036**.
20 A. Mukherjee, J. A. Okolie, A. Abdelrasoul, C. Niu and A. K. Dalai, *J. Environ. Sci.*, 2019, **83**, 46–63, DOI: **10.1016/j.jes.2019.03.014**.
21 M. K. Mondal, H. K. Balsora and P. Varshney, *Energy*, 2012, **46**(1), 431–441, DOI: **10.1016/j.energy.2012.08.006**.
22 N. A. Rashidi and S. Yusup, *J. CO2 Util.*, 2016, **13**, 1–16, DOI: **10.1016/j.jcou.2015.11.002**.
23 U. Khan, C. C. Ogbaga, O. A. A. Abiodun, A. A. Adeleke, P. P. Ikubanni, P. U. Okoye and J. A. Okolie, *Carbon*

Capture Sci. Technol., 2023, **8**, 100125, DOI: 10.1016/j.ccst.2023.100125.
24 J. D. Figueroa, T. Fout, S. Plasynski, H. McIlvried and R. D. Srivastava, *Int. J. Greenhouse Gas Control*, 2008, **2**(1), 9–20, DOI: 10.1016/S1750-5836(07)00094-1.
25 M. A. Nemitallah, M. A. Habib, H. M. Badr, S. A. Said, A. Jamal, R. Ben-Mansour, E. M. Mokheimer and K. Mezghani, *Int. J. Energy Res.*, 2017, **41**(12), 1670–1708, DOI: 10.1002/er.3722.
26 T. Mattisson and A. Lyngfelt, *Capture of CO_2 using chemical-looping combustion*, Scandinavian-Nordic Section of Combustion Institute, 2001, pp. 163–168.
27 A. Brunetti, F. Scura, G. Barbieri and E. Drioli, *J. Membr. Sci.*, 2010, **359**(1–2), 115–125, DOI: 10.1016/j.memsci.2009.11.040.
28 C. H. Yu, C. H. Huang and C. S. Tan, *Aerosol Air Qual. Res.*, 2012, **12**(5), 745–769, DOI: 10.4209/aaqr.2012.05.0132.
29 J. Y. Lai, L. H. Ngu and S. S. Hashim, *Greenhouse Gases: Sci. Technol.*, 2021, **11**(5), 1076–1117, DOI: 10.1002/ghg.2112.
30 Z. Yong, V. Mata and A. E. Rodrigues, *Sep. Purif. Technol.*, 2002, **26**(2–3), 195–205, DOI: 10.1016/S1383-5866(01)00165-4.
31 D. M. D'Alessandro, B. Smit and J. R. Long, *Angew. Chem., Int. Ed.*, 2010, **49**(35), 6058–6082, DOI: 10.1002/anie.201000431.
32 M. E. Davis, *Nature*, 2002, **417**(6891), 813–821, DOI: 10.1038/nature00785.
33 O. M. Yaghi, H. Li, C. Davis, D. Richardson and T. L. Groy, *Acc. Chem. Res.*, 1998, **31**(8), 474–484, DOI: 10.1021/ar970151f.
34 G. Férey, C. Mellot-Draznieks, C. Serre and F. Millange, *Acc. Chem. Res.*, 2005, **38**(4), 217–225, DOI: 10.1021/ar040163i.
35 S. Kitagawa, *Chem. Soc. Rev.*, 2014, **43**(16), 5415–5418, DOI: 10.1039/C4CS90059F.
36 S. Greed and O. M. Yaghi, *Nat. Rev. Chem.*, 2025, 1–3, DOI: 10.1038/s41570-025-00691-w.
37 O. M. Yaghi and H. Li, *J. Am. Chem. Soc.*, 1995, **117**(41), 10401–10402, DOI: 10.1021/ja00146a033.
38 V. Benoit, N. Chanut, R. S. Pillai, M. Benzaqui, I. Beurroies, S. Devautour-Vinot, C. Serre, N. Steunou, G. Maurin and P. L. Llewellyn, *J. Mater. Chem. A*, 2018, **6**(5), 2081–2090, DOI: 10.1039/C7TA09696H.
39 Y. Xue, G. Zhao, R. Yang, F. Chu, J. Chen, L. Wang and X. Huang, *Nanoscale*, 2021, **13**(7), 3911–3936, DOI: 10.1039/D0NR09064F.
40 C. Li, J. Hai, S. Li, B. Wang and Z. Yang, *Nanoscale*, 2018, **10**(18), 8667–8676, DOI: 10.1039/C8NR01487F.
41 N. Muzaffar, A. M. Afzal, H. H. Hegazy and M. W. Iqbal, *J. Energy Storage*, 2023, **64**, 107142, DOI: 10.1016/j.est.2023.107142.
42 M. G. Mohamed, A. F. El-Mahdy, M. G. Kotp and S. W. Kuo, *Mater. Adv.*, 2022, **3**(2), 707–733, DOI: 10.1039/D1MA00771H.
43 V. A. Davankov and M. P. Tsyurupa, *Angew. Makromol. Chem.*, 1980, **91**(1), 127–142, DOI: 10.1002/apmc.1980.050910111.
44 P. M. Budd, B. S. Ghanem, S. Makhseed, N. B. McKeown, K. J. Msayib and C. E. Tattershall, *Chem. Commun.*, 2004, **2**, 230–231, DOI: 10.1039/B311764B.
45 A. P. Cote, A. I. Benin, N. W. Ockwig, M. O'Keeffe, A. J. Matzger and O. M. Yaghi, *Science*, 2005, **310**(5751), 1166–1170, DOI: 10.1126/science.1120411.
46 J. X. Jiang, F. Su, A. Trewin, C. D. Wood, N. L. Campbell, H. Niu, C. Dickinson, A. Y. Ganin, M. J. Rosseinsky, Y. Z. Khimyak and A. I. Cooper, *Angew. Chem.*, 2007, **119**(45), 8728, DOI: 10.1002/anie.200701595.
47 T. Ben, H. Ren, S. Ma, D. Cao, J. Lan, X. Jing, W. Wang, J. Xu, F. Deng, J. M. Simmons, S. Qui and G. Zhu, *Angew. Chem., Int. Ed.*, 2009, **48**(50), 9457–9460, DOI: 10.1002/anie.200904637.
48 N. Hedin, L. Chen and A. Laaksonen, *Nanoscale*, 2010, **2**(10), 1819–1841, DOI: 10.1039/C0NR00042F.
49 Y. Zeng, R. Zou and Y. Zhao, *Adv. Mater.*, 2016, **28**(15), 2855–2873, DOI: 10.1002/adma.201505004.
50 A. A. Olajire, *J. CO2 Util.*, 2017, **17**, 137–161, DOI: 10.1016/j.jcou.2016.12.003.
51 Y. Song, Q. Sun, B. Aguila and S. Ma, *Adv. Sci.*, 2019, **6**(2), 1801410, DOI: 10.1002/advs.201801410.
52 K. Geng, T. He, R. Liu, S. Dalapati, K. T. Tan, Z. Li, S. Tao, Y. Gong, Q. Jiang and D. Jiang, *Chem. Rev.*, 2020, **120**(16), 8814–8933, DOI: 10.1021/acs.chemrev.9b00550.
53 F. Haase and B. V. Lotsch, *Chem. Soc. Rev.*, 2020, **49**(23), 8469–8500, DOI: 10.1039/D0CS01027H.
54 X. Feng, X. Ding and D. Jiang, *Chem. Soc. Rev.*, 2012, **41**(18), 6010–6022, DOI: 10.1039/C2CS35157A.
55 S. Kandambeth, K. Dey and R. Banerjee, *J. Am. Chem. Soc.*, 2018, **141**(5), 1807–1822, DOI: 10.1021/jacs.8b10334.
56 P. J. Waller, F. Gándara and O. M. Yaghi, *Acc. Chem. Res.*, 2015, **48**(12), 3053–3063, DOI: 10.1021/acs.accounts.5b00369.
57 M. S. Lohse and T. Bein, *Adv. Funct. Mater.*, 2018, **28**(33), 1705553, DOI: 10.1002/adfm.201705553.
58 W. Wang, H. Khan, H. Wu and Y. Wang, *Macromol. Rapid Commun.*, 2025, 2401065, DOI: 10.1002/marc.202401065.
59 A. R. Sujatha, A. Anil, P. D. Raju and C. V. Suneesh, *Chem. – Asian J.*, 2025, **20**(7), e202401434, DOI: 10.1002/asia.202401434.
60 F. Ma and L. Ye, *Front. Fuels*, 2024, **1**, 1320326, DOI: 10.3389/ffuel.2023.1320326.
61 B. Zhang, M. Wei, H. Mao, X. Pei, S. A. Alshmimri, J. A. Reimer and O. M. Yaghi, *J. Am. Chem. Soc.*, 2018, **140**(40), 12715–12719, DOI: 10.1021/jacs.8b08374.
62 Y. Su, Y. Wan, H. Xu, K. I. Otake, X. Tang, L. Huang, S. Kitagawa and C. Gu, *J. Am. Chem. Soc.*, 2020, **142**(31), 13316–13321, DOI: 10.1021/jacs.0c05970.
63 S. J. Rowan, S. J. Cantrill, G. R. Cousins, J. K. Sanders and J. F. Stoddart, *Angew. Chem., Int. Ed.*, 2002, **41**(6), 898–952, DOI: 10.1002/1521-3773(20020315)41:6%3C898::AID-ANIE898%3E3.0.CO;2-E.

64 L. Zhu and Y. B. Zhang, *Molecules*, 2017, **22**(7), 1149, DOI: **10.3390/molecules22071149**.
65 H. Furukawa and O. M. Yaghi, *J. Am. Chem. Soc.*, 2009, **131**(25), 8875–8883, DOI: **10.1021/ja9015765**.
66 H. Wei, S. Chai, N. Hu, Z. Yang, L. Wei and L. Wang, *Chem. Commun.*, 2015, **51**(61), 12178–12181, DOI: **10.1039/C5CC04680G**.
67 L. Stegbauer, K. Schwinghammer and B. V. Lotsch, *Chem. Sci.*, 2014, **5**, 2789–2793, DOI: **10.1039/C4SC00016A**.
68 P. F. Wei, M. Z. Qi, Z. P. Wang, S. Y. Ding, W. Yu, Q. Liu, L. K. Wang, H. Z. Wang, W. K. An and W. Wang, *J. Am. Chem. Soc.*, 2018, **140**(13), 4623–4631, DOI: **10.1021/jacs.8b00571**.
69 W. Huang, W. Zhang, S. Yang, L. Wang and G. Yu, *Small*, 2024, **20**(18), 2308019, DOI: **10.1002/smll.202308019**.
70 W. Zhang, L. G. Qiu, Y. P. Yuan, A. J. Xie, Y. H. Shen and J. F. Zhu, *J. Hazard. Mater.*, 2012, **221**, 147–154, DOI: **10.1016/j.jhazmat.2012.04.025**.
71 G. Das, B. P. Biswal, S. Kandambeth, V. Venkatesh, G. Kaur, M. Addicoat, H. S. Verma and R. Banerjee, *Chem. Sci.*, 2015, **6**, 3931–3939, DOI: **10.1039/C5SC00512D**.
72 G. Lin, H. Ding, D. Yuan, B. Wang and C. Wang, *J. Am. Chem. Soc.*, 2016, **138**(10), 3302–3305, DOI: **10.1021/jacs.6b00652**.
73 X. Liu, D. Huang, C. Lai, G. Zeng, L. Qin, H. Wang, H. Yi, B. Li, S. Liu, M. Zhang, R. Deng, Y. Fu, L. Li, W. Xue and S. Chen, *Chem. Soc. Rev.*, 2019, **48**(20), 5266–5302, DOI: **10.1039/C9CS00299E**.
74 A. K. Mohammed and D. Shetty, *Environ. Sci.: Water Res. Technol.*, 2021, **7**(11), 1895–1927, DOI: **10.1039/D1EW00408E**.
75 C. R. DeBlase, K. E. Silberstein, T. T. Truong, H. D. Abruña and W. R. Dichtel, *J. Am. Chem. Soc.*, 2013, **135**(45), 16821–16824, DOI: **10.1021/ja409421d**.
76 D. G. Wang, T. Qiu, W. Guo, Z. Liang, H. Tabassum, D. Xia and R. Zou, *Energy Environ. Sci.*, 2021, **14**(2), 688–728, DOI: **10.1039/D0EE02309D**.
77 Q. Fang, J. Wang, S. Gu, R. B. Kaspar, Z. Zhuang, J. Zheng, H. Guo, S. Qiu and Y. Yan, *J. Am. Chem. Soc.*, 2015, **137**(26), 8352–8355, DOI: **10.1021/jacs.5b04147**.
78 M. Li, Y. Peng, F. Yan, C. Li, Y. He, Y. Lou, D. Ma, Y. Li, Z. Shi and S. Feng, *New J. Chem.*, 2021, **45**(6), 3343–3348, DOI: **10.1039/D0NJ04941G**.
79 C. S. Karthik, T. Skorjanc and D. Shetty, *Mater. Horiz.*, 2024, **11**(9), 2077–2094, DOI: **10.1039/D3MH01698F**.
80 Q. Gao, L. Bai, X. Zhang, P. Wang, P. Li, Y. Zeng, R. Zou and Y. Zhao, *Chin. J. Chem.*, 2015, **33**(1), 90–94, DOI: **10.1002/cjoc.201400550**.
81 L. Wang, B. Dong, R. Ge, F. Jiang, J. Xiong, Y. Gao and J. Xu, *Microporous Mesoporous Mater.*, 2016, **224**, 95–99, DOI: **10.1016/j.micromeso.2015.11.030**.
82 D. A. Pyles, J. W. Crowe, L. A. Baldwin and P. L. McGrier, *ACS Macro Lett.*, 2016, **5**(9), 1055–1058, DOI: **10.1021/acsmacrolett.6b00486**.
83 W. Yu, S. Gu, Y. Fu, S. Xiong, C. Pan, Y. Liu and G. Yu, *J. Catal.*, 2018, **362**, 1–9, DOI: **10.1016/j.jcat.2018.03.021**.
84 H. Zhang, Z. Wang, S. Liu, W. Li, S. Wei, M. Wang, L. Zhang, W. Lyu, S. Liu and X. Lu, *Sep. Purif. Technol.*, 2025, **356**, 129897, DOI: **10.1016/j.seppur.2024.129897**.
85 H. M. El-Kaderi, J. R. Hunt, J. L. Mendoza-Cortés, A. P. Côté, R. E. Taylor, M. O'Keeffe and O. M. Yaghi, *Science*, 2007, **316**(5822), 268–272, DOI: **10.1126/science.1139915**.
86 P. Guan, J. Qiu, Y. Zhao, H. Wang, Z. Li, Y. Shi and J. Wang, *Chem. Commun.*, 2019, **55**(83), 12459–12462, DOI: **10.1039/C9CC05710B**.
87 Y. Ding, Y. Wang, Y. Su, Z. Yang, J. Liu, X. Hua and H. Wei, *Chin. Chem. Lett.*, 2020, **31**(1), 193–196, DOI: **10.1016/j.cclet.2019.05.012**.
88 R. A. Maia, F. L. Oliveira, V. Ritleng, Q. Wang, B. Louis and P. M. Esteves, *Chem. – Eur. J.*, 2021, **27**(30), 8048–8055, DOI: **10.1002/chem.202100478**.
89 M. Yin, L. Wang and S. Tang, *ACS Appl. Mater. Interfaces*, 2022, **14**(50), 55674–55685, DOI: **10.1021/acsami.2c18226**.
90 Y. He, Y. F. Liu, X. Shen, J. Zhao, L. Yang and R. Y. Zou, *ACS Appl. Polym. Mater.*, 2023, **5**(11), 9497–9504, DOI: **10.1021/acsapm.3c01950**.
91 Z. Zhou, T. Ma, H. Zhang, S. Chheda, H. Li, K. Wang, S. Ehrling, R. Giovine, C. Li, A. H. Alawadhi, M. M. Abduljawad, M. O. Alawad, L. Gagliardi, J. Sauer and O. M. Yaghi, *Nature*, 2024, 1–6, DOI: **10.1038/s41586-024-08080-x**.
92 H. Chen, J. Qin, X. Ruan, Q. Zhang, H. Zhu and S. Zhu, *Sep. Purif. Technol.*, 2025, **354**, 129378, DOI: **10.1016/j.seppur.2024.129378**.
93 S. Krishnan and C. V. Suneesh, *Mater. Today Commun.*, 2021, **27**, 102251, DOI: **10.1016/j.mtcomm.2021.102251**.
94 G. Chang, L. Yang, J. Yang, Y. Huang, K. Cao, J. Ma and D. Wang, *Polym. Chem.*, 2016, **7**(37), 5768–5772, DOI: **10.1039/C6PY01154C**.
95 L. Zou, Y. Sun, S. Che, X. Yang, X. Wang, M. Bosch, Q. Wang, H. Li, M. Smith, S. Yuan, Z. Perry and H. Zhou, *Adv. Mater.*, 2017, **29**(37), 1700229, DOI: **10.1002/adma.201700229**.
96 A. A. Abd, S. Z. Naji, A. S. Hashim and M. R. Othman, *J. Environ. Chem. Eng.*, 2020, **8**(5), 104142, DOI: **10.1016/j.jece.2020.104142**.
97 H. Zhang, L. M. Yang and E. Ganz, *ACS Sustainable Chem. Eng.*, 2020, **8**(38), 14616–14626, DOI: **10.1021/acssuschemeng.0c05951**.
98 N. T. T. Ha, H. T. Thao and N. N. Ha, *J. Mol. Graphics Modell.*, 2022, **112**, 108124, DOI: **10.1016/j.jmgm.2022.108124**.
99 M. He, H. Zhao, J. Jia, W. Zhou, Z. Wang, K. An, Y. Jiao, X. Yang, X. Zhang and T. Fan, *Environ. Res.*, 2025, **267**, 120701, DOI: **10.1016/j.envres.2024.120701**.
100 H. Veldhuizen, S. A. Butt, A. V. Leuken, B. Van Der Linden, W. Rook, S. Van Der Zwaag and M. A. Van Der Veen, *ACS Appl. Mater. Interfaces*, 2023, **15**(24), 29186–29194, DOI: **10.1021/acsami.3c04561**.
101 P. G. Boyd, A. Chidambaram, E. García-Díez, C. P. Ireland, T. D. Daff, R. Bounds, A. Gładysiak, P. Schouwink,

S. M. Moosavi, M. M. Maroto-Valer, J. A. Reimer, J. A. R. Navarro, T. K. Woo, S. Garcia, K. C. Stylianou and B. Smit, *Nature*, 2019, **576**(7786), 253–256, DOI: **10.1038/s41586-019-1798-7**.

102 Z. Ma, Z. Yang, H. Zhang and Z. Liu, *Microporous Mesoporous Mater.*, 2020, **296**, 109992, DOI: **10.1016/j.micromeso.2019.109992**.

103 S. K. S. Freitas, R. S. Borges, C. Merlini, G. M. O. Barra and P. M. Esteves, *J. Phys. Chem. C*, 2017, **121**(48), 27247–27252, DOI: **10.1021/acs.jpcc.7b10487**.

104 G. Singh, J. Lee, A. Karakoti, R. Bahadur, J. Yi, D. Zhao, K. AlBahily and A. Vinu, *Chem. Soc. Rev.*, 2020, **49**(13), 4360–4404, DOI: **10.1039/D0CS00075B**.

105 N. Huang, P. Wang, M. A. Addicoat, T. Heine and D. Jiang, *Angew. Chem.*, 2017, **129**(18), 5064–5068, DOI: **10.1002/ange.201611542**.

106 K. Su, W. Wang, J. Chang, E. S. M. El-Sayed, L. Zhang and D. Yuan, *CCS Chem.*, 2022, **4**(9), 3095–3105, DOI: **10.31635/ccschem.021.202101453**.

107 F. J. Uribe-Romo, C. J. Doonan, H. Furukawa, K. Oisaki and O. M. Yaghi, *J. Am. Chem. Soc.*, 2011, **133**(30), 11478–11481, DOI: **10.1021/ja204728y**.

108 J. Rouquerol, F. Rouquerol, P. Llewellyn, G. Maurin and K. Sing, *Adsorption by powders and porous solids: principles, methodology and applications*, Academic Press, 2nd edn, 2013.

109 K. Ariga, *Materials*, 2024, **17**(4), 936, DOI: **10.3390/ma17040936**.

110 K. Ariga, *ChemNanoMat*, 2023, **9**(7), e202300120, DOI: **10.1002/cnma.202300120**.

111 T. Banerjee, F. Haase, S. Trenker, B. P. Biswal, G. Savasci, V. Duppel, I. Moudrakovski, C. Ochsenfeld and B. V. Lotsch, *Nat. Commun.*, 2019, **10**(1), 2689, DOI: **10.1038/s41467-019-10574-6**.

112 Y. Meng, Y. Luo, J. L. Shi, H. Ding, X. Lang, W. Chen, A. Zheng, J. Sun and C. Wang, *Angew. Chem., Int. Ed.*, 2020, **59**(9), 3624–3629, DOI: **10.1002/anie.201913091**.

113 Y. Xie, J. Li, C. Lin, B. Gui, C. Ji, D. Yuan, J. Sun and C. Wang, *J. Am. Chem. Soc.*, 2021, **143**(19), 7279–7284, DOI: **10.1021/jacs.1c03042**.

114 T. Ma, E. A. Kapustin, S. X. Yin, L. Liang, Z. Zhou, J. Niu, L. H. Li, Y. Wang, J. Su, J. Li, X. Wang, W. D. Wang, W. Wang, J. Sun and O. M. Yaghi, *Science*, 2018, **361**(6397), 48–52, DOI: **10.1126/science.aat7679**.

115 X. Kang, X. Han, C. Yuan, C. Cheng, Y. Liu and Y. Cui, *J. Am. Chem. Soc.*, 2020, **142**(38), 16346–16356, DOI: **10.1021/jacs.0c06605**.

116 H. L. Nguyen, C. Gropp, Y. Ma, C. Zhu and O. M. Yaghi, *J. Am. Chem. Soc.*, 2020, **142**(48), 20335–20339, DOI: **10.1021/jacs.0c11064**.

117 H. Li, J. Ding, X. Guan, F. Chen, C. Li, L. Zhu, M. Xue, D. Yuan, V. Valtchev, Y. Yan, S. Qiu and Q. Fang, *J. Am. Chem. Soc.*, 2020, **142**(31), 13334–13338, DOI: **10.1021/jacs.0c06485**.

118 Z. Li, L. Sheng, C. Hsueh, X. Wang, H. Cui, H. Gao, Y. Wu, J. Wang, Y. Tang, H. Xu and X. He, *Chem. Mater.*, 2021, **33**(24), 9618–9623, DOI: **10.1021/acs.chemmater.1c03156**.

119 X. Xu, P. Cai, H. Chen, H. C. Zhou and N. Huang, *J. Am. Chem. Soc.*, 2022, **144**(40), 18511–18517, DOI: **10.1021/jacs.2c07733**.

120 W. Liu, L. Gong, Z. Liu, Y. Jin, H. Pan, X. Yang, B. Yu, N. Li, D. Qi, K. Wang, H. Wang and J. Jiang, *J. Am. Chem. Soc.*, 2022, **144**(37), 17209–17218, DOI: **10.1021/jacs.2c07596**.

121 F. Jin, E. Lin, T. Wang, S. Geng, L. Hao, Q. Zhu, Z. Wang, Y. Chen, P. Cheng and Z. Zhang, *J. Am. Chem. Soc.*, 2022, **144**(50), 23081–23088, DOI: **10.1021/jacs.2c10548**.

122 Z. Kahveci, T. Islamoglu, G. A. Shar, R. Ding and H. M. El-Kaderi, *CrystEngComm*, 2013, **15**(8), 1524–1527, DOI: **10.1039/C2CE26487K**.

123 C. Jia, R. R. Liang, S. X. Gan, S. Y. Jiang, Q. Y. Qi and X. Zhao, *Chem. – Eur. J.*, 2023, **29**(29), e202300186, DOI: **10.1002/chem.202300186**.

124 B. P. Biswal, S. Chandra, S. Kandambeth, B. Lukose, T. Heine and R. Banerjee, *J. Am. Chem. Soc.*, 2013, **135**(14), 5328–5331, DOI: **10.1021/ja4017842**.

125 S. Chandra, S. Kandambeth, B. P. Biswal, B. Lukose, S. M. Kunjir, M. Chaudhary, M. R. Babarao, T. Heine and R. Banerjee, *J. Am. Chem. Soc.*, 2013, **135**(47), 17853–17861, DOI: **10.1021/ja408121p**.

126 A. F. El-Mahdy, Y. H. Hung, T. H. Mansoure, H. H. Yu, Y. S. Hsu, K. C. Wu and S. W. Kuo, *J. Taiwan Inst. Chem. Eng.*, 2019, **103**, 199–208, DOI: **10.1016/j.jtice.2019.07.016**.

127 D. Kaleeswaran, P. Vishnoi and R. Murugavel, *J. Mater. Chem. C*, 2015, **3**(27), 7159–7171, DOI: **10.1039/C5TC00670H**.

128 H. Wang, D. Jiang, D. Huang, G. Zeng, P. Xu, C. Lai, M. Chen, M. Cheng, C. Zhang and Z. Wang, *J. Mater. Chem. A*, 2019, **7**(40), 22848–22870, DOI: **10.1039/C9TA06847C**.

129 S. Hug, L. Stegbauer, H. Oh, M. Hirscher and B. V. Lotsch, *Chem. Mater.*, 2015, **27**(23), 8001–8010, DOI: **10.1021/acs.chemmater.5b03330**.

130 J. Du, Y. Cui, Y. Liu, R. Krishna, Y. Yu, S. Wang, C. Zhang, X. Song and Z. Liang, *Microporous Mesoporous Mater.*, 2019, **276**, 213–222, DOI: **10.1016/j.micromeso.2018.10.001**.

131 Y. Zhang, Z. Chen, Q. Liu and J. Wan, *New J. Chem.*, 2022, **46**(10), 4555–4557, DOI: **10.1039/D2NJ00521B**.

132 Z. Li, X. Feng, Y. Zou, Y. Zhang, H. Xia, X. Liu and Y. Mu, *Chem. Commun.*, 2014, **50**(89), 13825–13828, DOI: **10.1039/C4CC05665E**.

133 N. Bagherian, A. R. Karimi and A. Amini, *Colloids Surf., A*, 2021, **613**, 126078, DOI: **10.1016/j.colsurfa.2020.126078**.

134 M. Zhang, R. Zheng, Y. Ma, R. Chen, X. Sun and X. Sun, *Microporous Mesoporous Mater.*, 2019, **285**, 70–79, DOI: **10.1016/j.micromeso.2019.04.021**.

135 J. L. Segura, M. J. Mancheño and F. Zamora, *Chem. Soc. Rev.*, 2016, **45**(20), 5635–5671, DOI: **10.1039/C5CS00878F**.

136 T. Huang, W. Zhang, S. Yang, L. Wang and G. Yu, *SmartMat*, 2024, **5**(6), e1309, DOI: **10.1002/smm2.1309**.

137 F. J. Uribe-Romo, J. R. Hunt, H. Furukawa, C. Klock, M. O'Keeffe and O. M. Yaghi, *J. Am. Chem. Soc.*, 2009, **131**(13), 4570–4571, DOI: **10.1021/ja8096256**.

138 X. Wang, H. Liu, J. Zhang and S. Chen, *Polym. Chem.*, 2023, **14**(12), 1293–1317, DOI: **10.1039/D2PY01350A**.
139 H. Li, A. Dilipkumar, S. Abubakar and D. Zhao, *Chem. Soc. Rev.*, 2023, **52**(18), 6294–6329, DOI: **10.1039/D2CS00465H**.
140 H. Wei, S. Chai, N. Hu, Z. Yang, L. Wei and L. Wang, *Chem. Commun.*, 2015, **51**(61), 12178–12181, DOI: **10.1039/C5CC04680G**.
141 S. Kandambeth, A. Mallick, B. Lukose, M. V. Mane, T. Heine and R. Banerjee, *J. Am. Chem. Soc.*, 2012, **134**(48), 19524–19527, DOI: **10.1021/ja308278w**.
142 N. Huang, X. Chen, R. Krishna and D. Jiang, *Angew. Chem., Int. Ed.*, 2015, **54**(10), 2986–2990, DOI: **10.1002/anie.201411262**.
143 R. Dawson, D. J. Adams and A. I. Cooper, *Chem. Sci.*, 2011, **2**(6), 1173–1177, DOI: **10.1039/C1SC00100K**.
144 S. Krishnan and C. V. Suneesh, *J. Photochem. Photobiol., A*, 2019, **371**, 414–422, DOI: **10.1016/j.jphotochem.2018.11.044**.
145 R. Gomes, P. Bhanja and A. Bhaumik, *Chem. Commun.*, 2015, **51**(49), 10050–10053, DOI: **10.1039/C5CC02147B**.
146 S. Wu, S. Gu, A. Zhang, G. Yu, Z. Wang, J. Jian and C. Pan, *J. Mater. Chem. A*, 2015, **3**(2), 878–885, DOI: **10.1039/C4TA04734F**.
147 H. Lyu, H. Li, N. Hanikel, K. Wang and O. M. Yaghi, *J. Am. Chem. Soc.*, 2022, **144**(28), 12989–12995, DOI: **10.1021/jacs.2c05382**.
148 Z. Li, L. Sheng, H. Wang, X. Wang, M. Li, Y. Xu, H. Cui, H. Zhang, H. Liang, H. Xu and X. He, *J. Am. Chem. Soc.*, 2020, **143**(1), 92–96, DOI: **10.1021/jacs.0c11313**.
149 Q. Zhu, X. Wang, R. Clowes, P. Cui, L. Chen, M. A. Little and A. I. Cooper, *J. Am. Chem. Soc.*, 2020, **142**(39), 16842–16848, DOI: **10.1021/jacs.0c07732**.
150 C. Gao, J. Li, S. Yin, G. Lin, T. Ma, Y. Meng, J. Sun and C. Wang, *Angew. Chem., Int. Ed.*, 2019, **58**(29), 9770–9775, DOI: **10.1002/anie.201905591**.
151 L. Zhang, D. Wang, M. Cong, X. Jia, Z. Liu, L. He, C. Li and Y. Zhao, *Chem. Commun.*, 2023, **59**(33), 4911–4914, DOI: **10.1039/D3CC00851G**.
152 F. Yuan, Z. Yang, X. Zhang, C. Tong, G. Gahungu, W. Li and J. Zhang, *J. Comput. Chem.*, 2021, **42**(13), 888–896, DOI: **10.1002/jcc.26510**.
153 S. Wei, H. Xin, M. Wang, S. Xu, W. Zhai, S. Liu, L. Wang, S. Liu, Z. Wang and X. Lu, *Adv. Theory Simul.*, 2022, **5**(12), 2200588, DOI: **10.1002/adts.202200588**.
154 B. Gui, G. Lin, H. Ding, C. Gao, A. Mal and C. Wang, *Acc. Chem. Res.*, 2020, **53**(10), 2225–2234, DOI: **10.1021/acs.accounts.0c00357**.
155 U. Khan, C. C. Ogbaga, O. A. O. Abiodun, A. A. Adeleke, P. P. Ikubanni, P. U. Okoye and J. A. Okolie, *Carbon Capture Sci. Technol.*, 2023, **8**, 100125, DOI: **10.1016/j.ccst.2023.100125**.